Far Infrared Light Irradiation Enhances Microglial Aβ Clearance and Ameliorates Cognitive Deficit in Alzheimer's Disease-like Mice

Zhi Wang (wangzhi@mail.sysu.edu.cn)
Department of Anesthesiology, Sun Yat-Sen Memorial Hospital, Sun Yat-Sun University.
https://orcid.org/0000-0002-0166-6109

Qingyong Li
Department of Anesthesiology, Sun Yat-Sen Memorial Hospital, Sun Yat-Sen University.

Wensi Wu
Department of Anesthesiology Sun Yat-Sen Memorial Hospital, Sun Yat-Sen University.

Yanan Lu
Department of Anesthesiology, Sun Yat-Sen Memorial Hospital, Sun Yat-Sen University.

Jing Wen
Department of Anesthesiology, Sun Yat-Sen Memorial Hospital, Sun Yat-Sen University.

Jiaoyan Ren
School of Food Science and Technology, South China University of Technology.

Huiying Zhao
Guangdong Provincial Key Laboratory of Malignant Tumor Epigenetics and Gene Regulation, Sun Yat-Sen Memorial Hospital, Sun Yat- Sen University.

Zhiyi Zuo
Department of Anesthesiology University of Virginia, Charlottesville.

Research

Keywords: Far infrared light, Alzheimer's disease, microglial phagocytosis, amyloid-β clearance, neuroinflammation

Posted Date: December 15th, 2020

DOI: https://doi.org/10.21203/rs.3.rs-125098/v1

Abstract

Background: Exposure to sunlight may decrease the risk of developing Alzheimer's disease (AD). However, the wavelength of the light with this therapeutic effect and the related mechanism remain elusive. Failure to clear amyloid-β (Aβ), the main component of amyloid plaque, has been considered as a key risk to cause the development of AD. As the resident immune cell in the brain, microglia is able to carry out Aβ clearance. We hypothesize that a component of sunlight improves AD-related cognitive dysfunction and that this beneficial effect may be via Aβ clearance by microglia.

Method: The APP/PS1 mice by 8.5 months of age were exposed to the visible light (λ = 500 nm), near infrared light (λ = 800 nm) and far infrared light (λ = 3 - 25 μm) for 60 min per day. After 5-week treatment with different light, all mice began to be subjected to Morris water maze behavior test under SPF environment. Western blotting was carried out to detect the expression of postsynaptic density-95 protein and synaptophysin in the hippocampus. The protein amount of interleukin (IL)-1β and IL-6 in the cerebral cortex were determined by using ELISA kits. Immunostaining was performed to characterize the Aβ, microglia, cluster of differentiation 68. Under the condition of Aβ existing, primary cultured microglia were treated with light for 2 h before Aβ phagocytosis assay.

Results: The APP/PS1 mice with different light (VIS, NIR and FIR) treatments showed a trend of improvement in learning compared to those without light treatment during training stage. Moreover, FIR light-treated APP/PS1 mice had better spatial memory than APP/PS1 mice in the probe test. Simultaneously, FIR light treatment restored synaptophysin protein expression, promoted the recruitment of microglia to Aβ plaques, enhanced the phagocytosis of Aβ, reduced Aβ burden and alleviated neuroinflammation.

Conclusions: Taken together, FIR light treatment ameliorates the learning and memory impairment in AD-like mice. Our findings uncovered a previously unappreciated function of FIR light, suggesting that FIR light treatment may be a potential therapeutic strategy for AD.

Introduction

Alzheimer's disease (AD) is the most common neurodegenerative disease in the elderly, and is characterized by the presence of amyloid plaques and neurofibrillary tangles and a progressive loss in memory and mental function[1, 2]. To date, there is no disease process-modifying intervention for AD [3]. It is estimated that more than 100 million people worldwide will live with AD by 2050[4], which will be an enormous burden on the family, caregivers and society. Therefore, the prevention and treatment of AD are urgently needed. One major theory is that the imbalance between amyloid-β (Aβ) production and clearance results in the accumulation and aggregation of Aβ, which lead to many pathological processes in AD pathology, including neuroinflammation, oxidative stress and synaptic deficit[5, 6]. Therefore, it has been a focus to find drugs that can eliminate the effects of Aβ. A large number of anti-Aβ drugs including semagacestat, bapineuzumab and solanezumab had been proceeded to clinical trials but most of them

had failed [7]. Various explanations for the failures have been suggested including side effect, neuroinflammation induction and wrong drug doses[7, 8]. Probably the most important reason is that the exact pathophysiology for AD remains not fully understood. Current drug therapies only treat symptoms rather than the underlying disease pathology[9].

Although the exact pathophysiology of AD remains unclear, it is widely recognized that the combination of genetic, environmental and lifestyle factors play an important role in AD progression. Interestingly, it was reported that exposure to sunlight could be linked to decreased risk of dementia[10]. Old people with non-melanoma skin cancer (NMSC) probably caused by overexposure to the sun had a markedly reduced risk of developing AD as compared to whom without NMSC[11]. Near infrared light irradiation could mitigate Alzheimer's disease-related pathology and synaptic vulnerability[12, 13]. Even ultraviolet radiation exposure was able to enhance learning and memory of mice[14]. These studies suggest that non-invasive photobiomodulation has a great potential in the treatment of AD. So far, pharmacological therapeutic strategies have not taken advantage of the brain's endogenous clearance mechanisms. As the resident immune cells in the brain, microglia are able to carry out Aβ clearance[15, 16]. However, very little is known on how to manipulate these cells for enhanced Aβ clearance due to the lack of noninvasive methods to measure this process[17]. It is worthwhile mentioning that sunlight has transcranial potential, especially for infrared light[18]. Based on the findings of its beneficial effects on dementia, sunlight exposure probably has a protective effect on brain cells, including microglia. Sunlight has three major components: ultraviolet light, visible light and infrared radiation[19]. However, which component of sunlight is most beneficial in reducing AD-related neuropathology and cognitive dysfunction and whether they affect the microglia for Aβ clearance remains unclear.

We hypothesize that a component of sunlight improves AD-related cognitive dysfunction and that this beneficial effect may be via Aβ clearance by microglia. To test these hypotheses, we investigated the effects of the visible light (λ = 500 nm), near infrared light (λ = 800 nm) and far infrared light (λ = 3–25 μm) on the cognitive ability of AD-like mice. We also determined whether the light with a potential to treat AD could affect microglial Aβ clearance.

Methods

Animals. The APP_{swe}/PSEN1dE9 double- transgenic (APP/PS1) and their littermate wild-type (WT) mice were obtained from Nanjing Biomedical Research Institute of Nanjing University (Nanjing, China). These mice were housed in specific pathogen free (SPF) environment with a 12-hour light/12-hour dark cycle. Mouse was caged singly and allowed to have food and water ad libitum. All experimental animal procedures were approved by the Institutional Animal Care and Use Committee (Approval No.: IACUC-20180918-010) and the Laboratory Animal Ethics Committee of Jinan University.

Light irradiation treatment. At the age of 8.5 months, APP/PS1 mice were randomly distributed to the following groups: sham treatment group, the visible light (λ = 500 nm) treatment group (VIS light-treated

APP/PS1 mice), the near infrared light (λ = 800 nm) treatment group (NIR light-treated APP/PS1 mice), and the far infrared light (the wavelength range was from 3 to 25 μm) treatment group (FIR light-treated APP/PS1 mice). A WT mouse group was also included. Mice in all groups were allowed free feeding during light irradiation that was 60 min per day for 1.5 months.

Morris water maze. After 5-week treatment with different light (VIS, NIR and FIR), all mice began to be subjected to Morris water maze behavior test under SPF environment. The Morris water maze experiment apparatus consisted of a circular pool with a diameter of 120 cm and a height of 50 cm, and water was injected into the pool. The camera was located just above the tank (connected to the computer), which was used to record the movement of mice. An appropriate amount of non-toxic protein powder was added into water to facilitate this recording. The pool temperature was maintained at 20–22 °C, and the water surface was divided into four quadrants (from one to four) and twelve zones (from one to twelve).

The water maze experiment was divided into two parts: the first is the training trial section (navigation stage of water maze), and the second is the spatial probe test (space memory stage). In the training trial, the target platform (8 cm in diameter, 20 cm in height) was located in the center between zone 2 and zone 6 in the second quadrant, and the water surface was 1 cm higher than the target platform, so that the mice could not see the platform. The experimental parameters were as follows: swimming time (60 s), residence time on target platform (3 s). During the water maze training trials, mice were placed into the water in accordance with the east and west directions. After mouse facing the pool wall into the water, the time required to find the target platform was recorded, namely escape latency. Mice were allowed to stand on the target platform for 10 s when climbing up to the target platform. However, if mice were unable to find the target platform within 60 s, they were manually guided to find the target platform, and allowed to stay on it for 15 s. Each training cycle was done for 4 times and for 7 continuous days. In the spatial probe test that was 24 h after the last training trial, the target platform was removed. Mice were placed into the water again and observed for a period of time (60 s). The number of entry into effective zones to find the target platform was recorded to reflect the spatial memory of mice.

Immunostaining. After the behavioral tests, the brain tissues of the mice were isolated and bisected longitudinally. The left hemisphere was frozen at -80 °C for further biochemical study. The right hemisphere was soaked in 4% paraformaldehyde solution for 24 h. Subsequently, they were immersed in 10%, 20% and 30% sucrose solutions each for 24 h and then stored in Tissue-Tek OCT compound at -20 °C. Coronal 30-μm thick sections from the right hemisphere were cut by a cryostat. The sections were washed with phosphate buffered saline (PBS).

For immunohistochemistry, the activity of endoperoxidase was blocked by 3% H_2O_2. Antigen retrieval with citric acid buffer (pH 6.0) was performed at 95 °C for 10 min. After washed with PBS, sections were incubated with 0.3% triton X-100 and 5% donkey serum for 60 min at room temperature. The sections were then incubated with mouse anti-Aβ antibody (1:10000, Sig-39300, Biolegend) overnight at 4 °C. Sections were then washed with PBS containing 0.3% triton x-100 and incubated with goat anti-mouse/rabbit IgG conjugated with horseradish peroxidase (Universal kit, PV-600, Zhongshan Jinqiao,

Beijing, China) at room temperature for 30 min. After washed with PBS, sections were incubated with hydrogen peroxide (DAB kit, Zhongshan Jinqiao) and co-stained with hematoxylin [E803FA0003, Sangon Biotech (Shanghai) Co., Ltd, China] at room temperature for 5 min. Images were captured using a Nikon microscope (Nikon Ni-U)

For immunofluorescent staining, after blocking with 0.3% triton X-100 and 5% donkey serum at room temperature for 60 min, sections were then incubated at 4 °C overnight with the following primary antibodies: mouse monoclonal anti-Aβ (6E10) antibody (1:10000, Sig-39300, Biolegend), rabbit polyclonal anti-ionized calcium binding adapter molecule 1 (Iba1) (1:1000, 019-19741, Wako) or rat polyclonal anti-cluster of differentiation 68 (CD68) (1:2000, ab53444, Abcam). Sections were rinsed with PBS containing 0.3% Triton X-100. The sections were incubated at room temperature for 2 h with fluorescent secondary antibodies as follows: donkey anti-mouse IgG antibody conjugated with Alexa Fluor 488 (1:200, A21202, Invitrogen), donkey anti-rat IgG antibody conjugated with Alexa Fluor 488 (1:200, A21208, Invitrogen), donkey anti-rabbit IgG antibody conjugated with Alexa Fluor 555 (1:200, A31572, Invitrogen) or donkey anti-mouse IgG antibody conjugated with Alexa Fluor 647 (1:200, A31571, Invitrogen). Afterwards, the sections were incubated with 4', 6-diamidino-2-phenylindole (DAPI, C0065, Solarbio) for 10 min to stain the nuclei. Images were acquired using ZEISS microscope (ZEISS Imager A2) or ZEISS confocal microscope (ZEISS LSM 800 with airyscan).

Aβ plaque-associated microglial analysis. The quantification of Aβ plaque-associated microglia was similar to the previously reported method with minor modification[20]. Within 20 μm range from the edge of an Aβ plaque, the number of Iba1 staining positive cells was manually counted. At least 100 plaques in the cerebral cortex region and 40 plaques in the hippocampus per group were quantified. For further analysis, plaques were divided into several groups according to their sizes (< 300, 300 to 600, 600 to 1200 and > 1200 μm^2). The percentage of microglial $CD68^+$ area was expressed as the co-staining area of $Iba1^+$ and $CD68^+$ divided by $Iba1^+$ area. To further analyze the proximal interaction of microglia with Aβ plaque, the percentage of the co-staining area of $6E10^+$ and $Iba1^+$ in total $6E10^+$ area was calculated. The co-staining area of $6E10^+$, $CD68^+$ and $Iba1^+$ divided by the total $6E10^+$ area was calculated to analyze the proximal interaction of $CD68^+$ cells with Aβ plaque.

Primary microglial culture. Primary microglial cultures were performed as previously described with slight modifications[21, 22]. Briefly, C57BL/6 mouse at postnatal 0 to 3 days was quickly immersed in 75% ethanol, and then the entire brain tissue was carefully removed with a sterile spatula. The olfactory bulbs, cerebellum and hind brain were dissected away, and the meninges were also removed. Subsequently, the cortical tissues were harvested, transferred to a 35-mm petri dish containing 2 mL Hanks' Balanced Salt Solution (HBSS) and minced into approximately 1 mm pieces by using sterile surgical scissors. The minced tissues were mechanically dissociated into suspension with a 1 mL pipette, and then filtered into a 50 mL conical tube by using a 40-μm mesh filter. The filtrated cell suspension was then transferred into a poly-L-lysine-coated T75 flask and cultured with Dulbecco's modified Eagle's medium (DMEM) (C1995500BT, Gibco) supplemented with 10% fetal bovine serum (FBS) (SFBE, Natocor). After 3 days,

medium was changed to that composed of 25 ng/mL granulocyte-macrophage colony-stimulating factor (GM-CSF) (415-ML-010, R&D system) and 10% FBS. After cultured for 12–14 days, microglial cells on top of the mixed glial cell layer were harvested by shaking the culture flask and were used for further experiment when their purity evaluated by Iba1 staining was over 95%.

Phagocytosis assay. The microglial phagocytosis of $A\beta_{1-42}$ was analyzed similarly to a previously reported method with slight modifications[23]. Briefly, fluorescein amidite-labeled $A\beta_{1-42}$ (FAM-$A\beta_{1-42}$) (AS-23525, Anaspec) was first aggregated at 37 °C for 24 h with agitation. Primary microglial cultures were seeded in the poly-L-lysine-coated 6-well plates at a density of 1×10^5 cells/cm^2 and then cultured overnight. After the cells were treated with FIR light for 1 h, the aggregated FAM-$A\beta_{1-42}$ was added into the culture medium with a final concentration of 0.8 μg/mL. The primary microglial cultures were continuously treated with FIR light for additional 2 h. FAM-$A\beta_{1-42}$-containing cultured medium was removed. Cultures were washed three times with PBS. Subsequently, the fluorescent images were randomly captured in three fields for each well by using an OLYMPUS microscope (OLYMPUS, IX71). For fluorescent intensity detection by flow cytometry, primary microglial cultures were digested with 0.25% trypsin-EDTA (25200056, Gibco), and then were centrifuged at 1500 g for 5 min at 4 °C and washed with PBS for three times. For the microscopic images, the green fluorescent intensity of internalized FAM-$A\beta_{1-42}$ in each well, which was captured under a green fluorescent protein channel, was quantified based on the mean of fluorescent intensity from three random fields by using ImageJ 1.52n. The results of three images were averaged to reflect the phagocytosis activity of the cells in the well. In the case of detection by flow cytometry, the green fluorescent intensity of internalized FAM-$A\beta_{1-42}$ from 10000 cells each sample was recorded under a FITC channel and then was expressed as the Geo mean for each sample. These measurements were performed by a person who was blind to group assignments. Finally, the green fluorescent intensity of treated samples was normalized to the mean fluorescent intensity of the control group without FIR light treatment.

Elisa assay. The protein amount of interleukin (IL)-1β and IL-6 in the cerebral cortex were determined by using ELISA kits (catalog No: E-EL-M0037c for IL-1β, Catalog No: E-EL-M0044c, Elabscience) according to the manufacture's instruction. Briefly, small pieces of the cerebral cortex of mice were weighted. The tissue was then homogenized in PBS on ice with protease inhibitor cocktail for general use (P1005, Beyotime) [tissue weight (g): PBS (mL) volume = 1:9]. Subsequently, the homogenates were centrifuged at 5000 g for 8 min at 4 °C. The amount of IL-1β and IL-6 in the supernatant was then determined. The final level of IL-1β and IL-6 was then normalized to its protein content determined by a BCA protein assay kit (P0010, Beyotime).

Western blot. The level of synaptic proteins postsynaptic density-95 protein (PSD-95) and synaptophysin in the hippocampus were determined by using Western blotting as previously described with slight modifications[24, 25]. The hippocampal tissues were homogenized in the RIPA lysis buffer (CW23335, CWBIOTECH) by using 1 mL insulin syringe on ice. Homogenates were centrifuged at 12000 g at 4 °C for 15 min. The supernatant was used for Western blotting. The protein content of each sample was

determined by the enhanced BCA protein assay kit (P0010, Beyotime). Twenty microgram protein per lane was electrophoresed on a 10% polyacrylamide gel and then transferred to a polyvinylidene fluoride (PVDF) membrane. The membrane was blocked by 5% nonfat milk at room temperature for 60 min and then incubated at 4 °C over night with the following primary antibodies: mouse monoclonal anti-PSD-95 antibody (1:1000, 75 – 028, NeuroMab), mouse monoclonal anti-synaptophysin (1:1000, MABN1193, EMD Millipore), or rabbit monoclonal anti-β-actin (1:1000, 8457s, Cell Signaling). After washed with Tris Buffered Saline Tween (Catalog No: T1081, Solarbio), the membranes were then incubated with corresponding secondary antibodies at room temperature for 2 h. The signal of protein band was visualized using NcmECL Ultra (Catalog No: P10200, Ncmbiotech). The protein band intensity of PSD-95 and synaptophysin was normalized to the corresponding band intensity of β-actin from the same sample.

Statistical analysis. All data were expressed as means ± S.E.M. The statistical analysis of results was performed by using GraphPad Prism version 7.0. The significant difference was assessed by unpaired t test, one-way or two-way ANOVA followed by Turkey's or Dunett multiple comparisons test. The data of training sessions in the Morris water maze test was analyzed by two-way repeated measures ANOVA. A p value < 0.05 was considered statistically significant difference.

Results

FIR light ameliorated cognitive dysfunction of AD-like mice. The time-course of the *in vivo* experiments is shown in Fig. 1A. The Morris water maze test consisted of two stages: training trials and spatial probe test (Fig. 1B). WT mice took shorter time than APP/PS1 mice to find the platform in the training trials of the test (Fig. 1C). This impaired learning in APP/PS1 mice was improved by the treatment of various wavelengths of light [$F(4, 203) = 4.113$, $p = 0.0032$]. Compared to APP/PS1 mice, FIR light-treated but not VIS light- or NIR light-treated APP/PS1 mice had more entries into the zones around the platform in the spatial probe test (Fig. 1D). Notably, there was no difference in swimming speed among WT mice and APP/PS1 mice treated with or without various lights (Fig. 1E). These results suggest that FIR light treatment improves spatial memory of AD-like mice.

FIR light enhanced the expression of synaptic protein in AD-like mice. The impairment of synaptic plasticity including the decreased expression of proteins in synapse is a common phenomenon in the progression of AD[26]. PSD-95 and synaptophysin are a pre- and post-synaptic protein, respectively, and play a pivotal role in regulating synaptic plasticity, which closely correlates with cognitive functions[27, 28]. Since the cognitive dysfunction of APP/PS1 mice was attenuated by FIR light, we next determined whether FIR light could influence the level of PSD-95 and synaptophysin in the hippocampus. The level of PSD-95 did not exhibit significant changes in APP/PS1 mice compared with WT mice. However, the level of synaptophysin was decreased in the APP/PS1 mice compared to the WT mice but this decrease was attenuated in APP/PS1 mice treated with FIR light (Figs. 2A to 2C). Therefore, these results suggest that FIR light treatment is beneficial to restore synaptic protein expression in AD-like mice.

FIR light promoted microglial recruitment around the Aβ plaque and enhanced Aβ phagocytosis in AD-like mice. As the resident immune cells in the brain, microglia participate in the clearance of Aβ[29]. In the present study, numerous microglial cells were recruited around the Aβ plaques (Fig. 3A). In the cortex region, FIR light treatment enhanced the recruitment of microglia surrounding the Aβ plaques (Figs. 3B and 3C). The number of microglial cells surrounding the Aβ plaques was increased with increased sizes of Aβ plaques. FIR light increased the number of microglial cells no matter which size of Aβ plaques was considered (Fig. 3D). Similar results were observed in the hippocampus (Figs. 3E to 3G).

To investigate whether the microglia surrounding the plaques could engulf Aβ to achieve Aβ clearance, co-immunostaining of Iba1, CD68 and Aβ were carried out and the $CD68^+$ microglial phagosomes and internalized Aβ were quantified. The results showed that the microglia around the Aβ plaque expressed the phagocytosis marker CD68 (Fig. 4A). Compared to the microglia in APP/PS1 mice, the microglia in the APP/PS1 mice with FIR light treatment significantly had increased CD68 expression (Fig. 4B). In addition, the interaction between microglial cells and Aβ was enhanced due to the increase in their contact area and phagocytic area in the FIR light-treated APP/PS1 mice (Figs. 4C and 4D). These results suggested that FIR light treatment promoted microglial Aβ phagocytosis and clearance. To further determine whether FIR light could increase Aβ phagocytosis, primary mouse microglial cultures were used to assess FAM-$Aβ_{1-42}$ uptake. The results showed that microglia could engulf FAM-$Aβ_{1-42}$ (Fig. 5A) and FIR light treatment markedly enhanced the microglial capacity to engulf FAM-$Aβ_{1-42}$ (Figs. 5B and 5C). These results were in agreement with the findings that FIR light was able to significantly increase Aβ phagocytosis by microglia in the APP/PS1 mice.

Together, these results suggest that FIR light treatment increases microglial recruitment to the plaques and enhances microglial phagocytosis, which is beneficial to clean Aβ in the AD-like mice.

FIR light alleviated Aβ burden in the brain of AD-like mice. The Aβ accumulation and aggregation are mainly resulted from the imbalance of Aβ production and clearance and result in a series of subsequent pathological events for AD progression[5, 6]. Since there was a significant enhancement of microglial phagocytosis of Aβ in the APP/PS1 mice treated with FIR light, we next determined whether FIR light could reduce the Aβ load in the AD-like mice. Compared to WT mouse, APP/PS1 mouse exhibits abundant Aβ plaque in both cerebral cortex and hippocampus (Fig. 6A). A significant reduction of Aβ plaque in these brain areas of the FIR light-treated APP/PS1-mice was found compared to the APP/PS1 mice (Figs. 6B to 6G). These results indicate that FIR light treatment significantly reduces Aβ load in the brain of APP/PS1 transgenic mice.

FIR light decreased neuroinflammation in AD-like mice. Neuroinflammation mainly resulted from abnormal activation of microglia and astrocytes has been observed in the AD-like mouse brains and patients with AD[30]. Neuroinflammation can cause neuronal damage[30]. Thus, we determined whether FIR light treatment could alleviate neuroinflammation in the AD-like mice. The pro-inflammatory factors including IL-1β and IL-6 were significantly higher in the APP/PS1 mice compared to WT mice (Figs. 7A

and 7B). However, they were markedly reduced in the FIR light-treated APP/PS1 mice. These results suggest that FIR light treatment is able to alleviate neuroinflammation in the AD-like mice.

Discussion

With the increased life expectancy, much attention had been paid to the treatment of AD. During the progression of AD, the most common symptom is the decline in cognitive function including poor memory and learning skill. Accordingly, improving cognitive dysfunction has been a goal of AD treatment. Interestingly, it has been reported that sunlight exposure could decrease the risk of developing AD[10, 11]. Sunlight mainly contains three lights, namely ultraviolet light, visible light and infrared radiation[19]. In the present study, VIS light (λ = 500 nm), NIR light (λ = 800 nm) and FIR light (λ = 3–25 nm) were tested as a treatment strategy. APP/PS1 mice with different light treatments showed a trend of improvement in learning compared to those without light treatment during training stage. Notably, FIR light-treated APP/PS1 mice had better spatial memory than APP/PS1 mice in the probe test, indicating that FIR light treatment may have potential to be a therapeutic strategy for AD.

The potential of using light as an AD treatment had been investigated. VIS light was found to inhibit the aggregation of Aβ under *in vitro* condition[31]. Photobiomodulation with NIR light attenuated AD-related pathology in K3 mice (aged 5 months) and APP/PS1 mice (aged 7 months)[12]. In the present study, we compared the effects of VIS, NIR and FIR light on the cognition function of the 8.5-month-old APP/PS1 mice that start to have cognition deficits by 6 months of age[32]. Only FIR light improved the spatial memory in APP/PS1 mice. FIR light irradiation that can penetrate up to 1.5 inches beneath the skin had been reported to have many positive biological effects in animals or humans, including improving blood circulation, ameliorating endothelial dysfunction, relieving fatigue and pain, lowering blood pressure, and promoting capillary dilation[33, 34]. The current study shows for the first time the beneficial effects of FIR light on the AD-like mice, such as improved cognitive function, restored the expression of the synaptic protein synaptophysin, reduced Aβ plaque burden in the cerebral cortex and hippocampus and decreased neuroinflam- mation.

Significant Aβ accumulation is a character of AD brain. Excessive Aβ has been hypothesized to drive the neuropathogenic cascades of AD including neuroinflammation, oxidative stress and synaptic failure [35, 36]. Reducing excessive Aβ in the brain has been proposed to be a potential treatment strategy for AD. Previous studies also showed that NIR light could reduce Aβ burden in the brain of AD mice[12, 13]. However, the mechanisms underlying these effects remain to be fully elucidated. As the resident immune cells in brain, microglia may be the first responder to clean Aβ through phagocytosis[29]. Accordingly, we try to focus on the involvement of microglia in the underlying mechanism for FIR light to decrease Aβ burden in the brain of AD mice. It is known that the phagocytosis ability of microglia decreases with age, leading to the reduction of Aβ clearance during AD development[37]. In the current study, FIR light enhanced microglial phagocytosis of Aβ. FIR light promoted the recruitment of microglia to Aβ plaque

with increased $CD68^+$ phagosomes in the APP/PS1 mice and enhanced microglial Aβ engulfment in mouse brain and primary microglial cultures.

Therefore, this finding is in agreement with the result that FIR light was able to reduce Aβ plaque burden in the cerebral cortex and hippocampus of APP/PS1 mice. Namely, FIR light treatment may act on microglia to reduce the deposition of Aβ in the brain of AD-like mice.

Although the microglial recruitment to Aβ and phagocytosis of Aβ in APP/PS1 mice were enhanced after FIR light treatment, the exact mechanism of these FIR light biological effects on microglia remains poorly understood. Previous study showed that NIR light can be absorbed by mitochondrial chromophores, such as cytochrome c oxidase (COX)[38]. This photon absorption possibly promotes the dissociation of the inhibitory molecule, NO, from the copper B site, resulting in the activation of the enzyme[39]. The loss of NO will rapidly lead to the increase in electron transport, oxygen consumption, and adenosine triphosphate (ATP) production[34, 39]. Consequently, signaling pathways will be activated and involved in the activation of transcription factors, such as nuclear factor-κB[40]. However, the principle chromophore at FIR light wavelengths is not COX but rather water[34]. Possible concept is that the nanometer water layers exist in the hydrophobic surfaces, such as cellular and mitochondrial membranes, and FIR light can perturb the structure of membrane underlying the nanoscopic water layers, resulting in the open of ion channels in the membrane and then possibly enhancing the mitochondrial respiration activity[34, 41]. Nevertheless, it cannot be excluded that FIR light may directly influence the COX activity[42, 43].

Microglial phagocytosis requires dynamic reorganization of the actin cytoskeleton, for which a substantial amount of ATP are necessary[44]. However, microglia in response to cerebral Aβ deposition will had a metabolic switch to glycolysis[45], which produces much lower amounts of ATP per glucose molecule than the oxidative metabolism modulated by mitochondrial respiratory activity[46]. Accordingly, we speculate that FIR light treatment promotes the microglial recruitment to Aβ and phagocytosis of Aβ through enhancing mitochondrial respiratory activity, which needs further systemic experiments to support this speculation. In addition, it is noteworthy that abnormally active microglia will release pro-inflammatory cytokines to cause neuronal damage[47]. However, glycolytic switch of microglia in response to cerebral Aβ deposition would promote pro-inflammatory state change, which could be blocked by inhibition of glycolysis[48]. In the present study, we observed that FIR light treatment significantly decreased pro-inflammatory cytokines, such as IL-1β and IL-6, in APP/PS1 mice. This phenomenon may be explained that FIR light treatment inhibits glycolysis switch and enhances mitochondrial oxidative phosphorylation, which would be consistent with the above speculation that FIR light treatment could enhance mitochondrial respiratory activity.

Previous studies suggest that proper neuronal function is the underlying mechanism for cognitive ability[49–51]. However, the excessive Aβ and the pro-inflammatory cytokines will cause neuronal damage [35, 36, 47], leading to synaptic function impairment. Synaptic plasticity deficit with decreased expression of synaptic protein can compromise normal neuronal functions, resulting in cognitive dysfunction, which

often occurs in the AD brain[27, 52]. In the present study, we found that APP/PS1 mice treated with FIR light had higher expression of synaptophysin than those without FIR light treatment. This result may possibly be a subsequence of the decrease in Aβ and proinflammatory cytokines after FIR light treatment. Together, our results suggest that FIR light treatment may normalize synaptic integrity, which may be a mechanism for the improved cognitive function of AD-like mice.

Limitations

Firstly, the design that wavelength of 500 nm, 800 nm and 3–25 μm represents as VIS, NIR and FIR light, respectively, is an over-simplification, while their wavelengths all cover extremely broad range[34]. So it needs tremendous workload to investigate the effect of different wavelength of light on cognitive function of AD-like mice. Secondly, the complexity of illumination parameters such as wavelength, fluence, power density, pulse structure and treatment timing also challenge the rational choose, which may lead to the publication of both negative and positive studies[53]. Therefore, we have not studied in detail the effects of different wavelength of light on cognitive function of AD-like mice. Thirdly, the APP/PS1 two transgenic mouse occur increased Aβ and amyloid plaque by the age of 4 months and cognitive deficits by the age of 6 months[32, 54]. However, the APP/PS1 mice acted as AD-like mice employed in the current study began to be subjected to FIR light treatment by 8.5 months of age. At this point in time, they were on the progressive stage of disease. In order to explore the effectiveness of FIR light treatment in more depth, further studies should consider the FIR light treatment strategy of AD-like mice in different age phase, such as 4-month-old and 6-month-old.

In the present study, we mainly focused on the effect of FIR light on the microglia, which would enhance the phagocytosis and clearance of Aβ. In addition to microglia, astrocyte similarly engaged in the process of AD development[55]. Activated astrocytes surrounding the Aβ neprilysin, an amyloid-degrading enzyme[56]. Functional experiment also suggested that astrocytes were able to phagocyte Aβ[57]. Simultaneously, astrocytes in conditions of AD-like pathology were observed to express β-site APP-cleaving enzyme 1, an important endoprotease for production of Aβ, thereby acquiring the ability to produce Aβ[58]. It was known that Aβ could remodel the astroglial glucose metabolism that involved in the ATP production and release[59, 60], which would mediate the chemotactic response of microglia[61]. In light of the pivotal role of astrocyte in the Aβ-induced condition, the further studies on functional changes of astrocyte under FIR light irradiation should be taken into consideration. It should be pointed out that FIR light might directly act on the neuron and influence Aβ-induced synaptic dysfunction. Accordingly, the functional changes of neuron and synaptic plasticity after FIR light treatment should not be ignored in the future studies.

Beyond the limitation mentioned above, the mechanism for how FIR light ameliorated cognitive dysfunction of AD-like mice has not been clearly defined although FIR light could enhance microglial Aβ phagocytosis and reduce Aβ burden in the brain of AD-like mice, subsequently contributing to the beneficial effect on synaptic plasticity and cognitive function. However, it could not be ruled out that FIR

probably had peripheral effects after FIR light irradiations of whole-body without making a distinction between head and body. Previous work by others showed that moderate UV light exposure could elevate blood urocanic acid (UAC)[14]. After crossing the blood-brain barrier (BBB), UAC was able to be converted to glutamate through intra-neuronal metabolic pathway. Such UV-triggered glutamate synthesis could contribute to some of neurobehavioral changes. Therefore, further studies should assess the potential FIR light-induced peripheral molecule that could across BBB and then directly or indirectly regulate the neurobehavioral function.

Lastly, the molecules and pathways mediating the biological effects of FIR light on microglia, especially for the mechanism underlying enhanced microglial phagocytosis of Aβ after FIR light treatment, should be well studied.

Conlusion

In summary, we found that FIR light at wavelengths of 3–25 μm significantly promoted recruitment of microglia to the Aβ plaque, enhanced the phagocytosis of Aβ by microglia, reduced Aβ burden, decreased neuroinflammatory cytokines and restored the expression of synaptic protein in AD-like mice. FIR light treatment also ameliorated the learning and memory impairment of these mice. These results suggest the therapeutic potential of FIR light for AD. Further study is needed to determine this potential and the molecular mechanisms for the protective effects of FIR light.

Abbreviations

AD: Alzheimer’s disease

FIR: far infrared

VIS: Visible light

NIR: Near infrared

Aβ: Amyloid-β

NMSC: Non-melanoma skin cancer

APP/PS1: APPswe/PSEN1dE9

WT: Wild-type

SPF: Specific pathogen free

PBS: Phosphate buffered saline

Iba1: Ionized calcium binding adapter molecule 1

CD68: cluster of differentiation 68

DAPI: 2-(4-Amidinophenyl)-6-indolecarbamidine dihydrochloride

HBSS: Hanks' Balanced Salt Solution

DMEM: Dulbecco’s modified Eagle’s medium

GM-CSF: Granulocyte-macrophage colony-stimulating factor

FBS: Fetal bovine serum

FAM-Aβ1-42: Fluorescein amidite-labeled Aβ1-42

IL-1β: interleukin-1β

IL-6: interleukin-6

PSD-95: Postsynaptic density-95 protein

PVDF: Polyvinylidene fluoride

COX: Cytochrome c oxidase

ATP: Adenosine triphosphate

UAC: Urocanic acid

BBB: Blood-brain barrier

Declarations

Ethics approval and consent to participate

All experimental animal procedures were approved by the Institutional Animal Care and Use Committee (Approval No.: IACUC-20180918-010) and the Laboratory Animal Ethics Committee of Jinan University.

Consent for publication

Written informed consent for publication was obtained from all participants.

Availability of data and materials

All data in this manuscript are available on reasonable request.

Competing interests:

The authors declare no competing financial interests

Funding:

This work was supported by grants from the National Natural Science Foundation of China (82002389 to QL and 81571196 to ZW), grants from Guangdong Science and Technology Department (2019A1515012147 to ZW), and a grant (201704020222) from Guangzhou Science, Technology and Innovation Commission, Guangzhou, China.

Authors' contributions

QL conceived and conducted most of the experiments, and wrote most of the manuscript. ZW conceived the idea for the project, coordinated the research and modified the manuscript with ZZ and WW. JR did much work to improved quality of our work such as revising the paper meticulously, providing a professional editing. HZ analyzed the results. YL and JW collected the data.

Acknowledgements:

We gratefully acknowledge the Guangdong Junfeng BFS Technology Co., Ltd for kindly providing related instruments.

References

1. Scheltens P, Blennow K, Breteler M M B, et al. Alzheimer's disease. The Lancet, 2016, 388(10043): 505-517.
2. De Lau L M, Breteler M M. Epidemiology of Parkinson's disease. The Lancet Neurology, 2006, 5(6): 525-535.
3. Gauthier S, Albert M, Fox N, et al. Why has therapy development for dementia failed in the last two decades? Alzheimer's & dementia: the journal of the Alzheimer's Association, 2016, 12(1): 60-64.
4. Prince M, Wimo A, Guerchet M, et al. Alzheimer’s Disease International: World Alzheimer Report 2015: The Global Impact of Dementia. Published by Alzheimer’s Disease International (ADI), London, 2015, 1-92.
5. Liu C-C, Zhao N, Yamaguchi Y, et al. Neuronal heparan sulfates promote amyloid pathology by modulating brain amyloid-β clearance and aggregation in Alzheimer’s disease. Science translational medicine, 2016, 8(332): 332ra44-332ra44.
6. Mawuenyega K G, Sigurdson W, Ovod V, et al. Decreased clearance of CNS β-amyloid in Alzheimer’s disease. Science, 2010, 330(6012): 1774-1774.
7. Anderson R M, Hadjichrysanthou C, Evans S, et al. Why do so many clinical trials of therapies for Alzheimer's disease fail? The Lancet, 2017, 390(10110): 2327-2329.
8. Doody R, Thomas R, Farlow M, et al. Alzheimer’s Disease Cooperative Study Steering Committee; Solanezumab study group. Phase 3 trials of solanezumab for mild-to-moderate Alzheimer’s disease.

N Engl J Med, 2014, 370(4): 311-321.
9. Diling C, Tianqiao Y, Jian Y, et al. Docking studies and biological evaluation of a potential β-secretase inhibitor of 3-hydroxyhericenone F from Hericium erinaceus. Frontiers in pharmacology, 2017, 8(219.
10. Littlejohns T J, Henley W E, Lang I A, et al. Vitamin D and the risk of dementia and Alzheimer disease. Neurology, 2014, 83(10): 920-928.
11. White R S, Lipton R B, Hall C B, et al. Nonmelanoma skin cancer is associated with reduced Alzheimer disease risk. Neurology, 2013, 80(21): 1966-1972.
12. Purushothuman S, Johnstone D M, Nandasena C, et al. Photobiomodulation with near infrared light mitigates Alzheimer's disease-related pathology in cerebral cortex–evidence from two transgenic mouse models. Alzheimer's research & therapy, 2014, 6(1): 1-13.
13. Comerota M M, Krishnan B, Taglialatela G. Near infrared light decreases synaptic vulnerability to amyloid beta oligomers. Scientific Reports, 2017, 7(1): 15012.
14. Zhu H, Wang N, Yao L, et al. Moderate UV Exposure Enhances Learning and Memory by Promoting a Novel Glutamate Biosynthetic Pathway in the Brain. Cell, 2018, 173(7): 1716-1727. e17.
15. Wyss-Coray T, Lin C, Yan F, et al. TGF-β1 promotes microglial amyloid-β clearance and reduces plaque burden in transgenic mice. Nature medicine, 2001, 7(5): 612-618.
16. Hickman S, Izzy S, Sen P, et al. Microglia in neurodegeneration. Nature neuroscience, 2018, 21(10): 1359-1369.
17. Singer A C, Martorell A J, Douglas J M, et al. Noninvasive 40-Hz light flicker to recruit microglia and reduce amyloid beta load. Nature protocols, 2018, 13(8): 1850.
18. De Taboada L, Yu J, El-Amouri S, et al. Transcranial laser therapy attenuates amyloid-β peptide neuropathology in amyloid-β protein precursor transgenic mice. Journal of Alzheimer's disease, 2011, 23(3): 521-535.
19. Sklar L R, Almutawa F, Lim H W, et al. Effects of ultraviolet radiation, visible light, and infrared radiation on erythema and pigmentation: a review. Photochemical & Photobiological Sciences, 2013, 12(1): 54-64.
20. Shi Q, Chowdhury S, Ma R, et al. Complement C3 deficiency protects against neurodegeneration in aged plaque-rich APP/PS1 mice. Science Translational Medicine, 2017, 9(392): eaaf6295.
21. Atagi Y, Liu C-C, Painter M M, et al. Apolipoprotein E is a ligand for triggering receptor expressed on myeloid cells 2 (TREM2). Journal of Biological Chemistry, 2015, 290(43): 26043-26050.
22. Zhong L, Wang Z, Wang D, et al. Amyloid-beta modulates microglial responses by binding to the triggering receptor expressed on myeloid cells 2 (TREM2). Molecular neurodegeneration, 2018, 13(1): 15.
23. Xiang X, Werner G, Bohrmann B, et al. TREM2 deficiency reduces the efficacy of immunotherapeutic amyloid clearance. EMBO molecular medicine, 2016, 8(9): 992-1004.
24. Lin D, Feng C, Cao M, et al. Volatile anesthetics may not induce significant toxicity to human neuron-like cells. Anesthesia & Analgesia, 2011, 112(5): 1194-1198.

25. Choi S H, Bylykbashi E, Chatila Z K, et al. Combined adult neurogenesis and BDNF mimic exercise effects on cognition in an Alzheimer's mouse model. Science, 2018, 361(6406): eaan8821.
26. Coleman P, Federoff H, Kurlan R. A focus on the synapse for neuroprotection in Alzheimer disease and other dementias. Neurology, 2004, 63(7): 1155-1162.
27. Zhang W, Gu G J, Zhang Q, et al. NSCs promote hippocampal neurogenesis, metabolic changes and synaptogenesis in APP/PS1 transgenic mice. Hippocampus, 2017, 27(12): 1250-1263.
28. Almeida C G, Tampellini D, Takahashi R H, et al. Beta-amyloid accumulation in APP mutant neurons reduces PSD-95 and GluR1 in synapses. Neurobiology of disease, 2005, 20(2): 187-198.
29. Fu A K, Hung K-W, Yuen M Y, et al. IL-33 ameliorates Alzheimer's disease-like pathology and cognitive decline. Proceedings of the National Academy of Sciences, 2016, 113(19): E2705-E2713.
30. Heneka M T, Carson M J, El Khoury J, et al. Neuroinflammation in Alzheimer's disease. The Lancet Neurology, 2015, 14(4): 388-405.
31. Lee J S, Lee B I, Park C B. Photo-induced inhibition of Alzheimer's β-amyloid aggregation in vitro by rose bengal. Biomaterials, 2015, 38(43-49.
32. Cao D, Lu H, Lewis T L, et al. Intake of sucrose-sweetened water induces insulin resistance and exacerbates memory deficits and amyloidosis in a transgenic mouse model of Alzheimer disease. Journal of Biological Chemistry, 2007, 282(50): 36275-36282.
33. Shui S, Wang X, Chiang J Y, et al. Far-infrared therapy for cardiovascular, autoimmune, and other chronic health problems: A systematic review. Experimental Biology and Medicine, 2015, 240(10): 1257-1265.
34. Vatansever F, Hamblin M R. Far infrared radiation (FIR): its biological effects and medical applications. Photonics & lasers in medicine, 2012, 1(4): 255-266.
35. Hardy J, Selkoe D J. The amyloid hypothesis of Alzheimer's disease: progress and problems on the road to therapeutics. science, 2002, 297(5580): 353-356.
36. Selkoe D J, Hardy J. The amyloid hypothesis of Alzheimer's disease at 25 years. EMBO molecular medicine, 2016, 8(6): 595-608.
37. Hickman S E, Allison E K, El Khoury J. Microglial dysfunction and defective β-amyloid clearance pathways in aging Alzheimer's disease mice. Journal of Neuroscience, 2008, 28(33): 8354-8360.
38. Eells J T, Wong-Riley M T, VerHoeve J, et al. Mitochondrial signal transduction in accelerated wound and retinal healing by near-infrared light therapy. Mitochondrion, 2004, 4(5-6): 559-567.
39. Lane N. Cell biology: power games. Nature, 2006, 443(7114): 901-903.
40. Chen A C, Arany P R, Huang Y-Y, et al. Low-level laser therapy activates NF-kB via generation of reactive oxygen species in mouse embryonic fibroblasts. PloS one, 2011, 6(7): e22453.
41. Sommer A P, Caron A, Fecht H-J. Tuning nanoscopic water layers on hydrophobic and hydrophilic surfaces with laser light. Langmuir, 2008, 24(3): 635-636.
42. Rich P R, Breton J. Attenuated total reflection Fourier transform infrared studies of redox changes in bovine cytochrome c oxidase: Resolution of the redox Fourier transform infrared difference spectrum

of heme a 3. Biochemistry, 2002, 41(3): 967-973.
43. Heitbrink D, Sigurdson H, Bolwien C, et al. Transient binding of CO to CuB in cytochrome c oxidase is dynamically linked to structural changes around a carboxyl group: a time-resolved step-scan Fourier transform infrared investigation. Biophysical journal, 2002, 82(1): 1-10.
44. Engl E, Attwell D. Non-signalling energy use in the brain. The Journal of physiology, 2015, 593(16): 3417-3429.
45. Wendeln A-C, Degenhardt K, Kaurani L, et al. Innate immune memory in the brain shapes neurological disease hallmarks. Nature, 2018, 556(7701): 332-338.
46. Mookerjee S A, Gerencser A A, Nicholls D G, et al. Quantifying intracellular rates of glycolytic and oxidative ATP production and consumption using extracellular flux measurements. Journal of Biological Chemistry, 2017, 292(17): 7189-7207.
47. Calsolaro V, Edison P. Neuroinflammation in Alzheimer's disease: Current evidence and future directions. Alzheimer's & Dementia, 2016, 12(6): 719-732.
48. Bennett F C, Liddelow S A. Microglia Metabolic Breakdown Drives Alzheimer's Pathology. Cell metabolism, 2019, 30(3): 405-406.
49. Scheff S, Price D, Schmitt F, et al. Synaptic alterations in CA1 in mild Alzheimer disease and mild cognitive impairment. Neurology, 2007, 68(18): 1501-1508.
50. Dickson D W, Crystal H A, Bevona C, et al. Correlations of synaptic and pathological markers with cognition of the elderly. Neurobiology of aging, 1995, 16(3): 285-298.
51. Selkoe D J. Alzheimer's disease is a synaptic failure. Science, 2002, 298(5594): 789-791.
52. Xu Y-J, Mei Y, Shi X-Q, et al. Albiflorin ameliorates memory deficits in APP/PS1 transgenic mice via ameliorating mitochondrial dysfunction. Brain research, 2019, 1719(113-123.
53. Sommer A P, Pinheiro A L, Mester A R, et al. Biostimulatory windows in low-intensity laser activation: lasers, scanners, and NASA's light-emitting diode array system. Journal of clinical laser medicine & surgery, 2001, 19(1): 29-33.
54. Garcia-Alloza M, Robbins E M, Zhang-Nunes S X, et al. Characterization of amyloid deposition in the APPswe/PS1dE9 mouse model of Alzheimer disease. Neurobiology of disease, 2006, 24(3): 516-524.
55. Verkhratsky A, Olabarria M, Noristani H N, et al. Astrocytes in Alzheimer's disease. Neurotherapeutics, 2010, 7(4): 399-412.
56. Apelt J, Ach K, Schliebs R. Aging-related down-regulation of neprilysin, a putative β-amyloid-degrading enzyme, in transgenic Tg2576 Alzheimer-like mouse brain is accompanied by an astroglial upregulation in the vicinity of β-amyloid plaques. Neuroscience letters, 2003, 339(3): 183-186.
57. Wyss-Coray T, Loike J D, Brionne T C, et al. Adult mouse astrocytes degrade amyloid-β in vitro and in situ. Nature medicine, 2003, 9(4): 453-457.
58. Roßner S, Lange-Dohna C, Zeitschel U, et al. Alzheimer's disease β-secretase BACE1 is not a neuron-specific enzyme. Journal of neurochemistry, 2005, 92(2): 226-234.

59. Soucek T, Cumming R, Dargusch R, et al. The regulation of glucose metabolism by HIF-1 mediates a neuroprotective response to amyloid beta peptide. Neuron, 2003, 39(1): 43-56.
60. Le Douce J, Maugard M, Veran J, et al. Impairment of glycolysis-derived L-serine production in astrocytes contributes to cognitive deficits in Alzheimer's disease. Cell metabolism, 2020, 31(3): 503-517. e8.
61. Davalos D, Grutzendler J, Yang G, et al. ATP mediates rapid microglial response to local brain injury in vivo. Nature neuroscience, 2005, 8(6): 752-758.

Figures

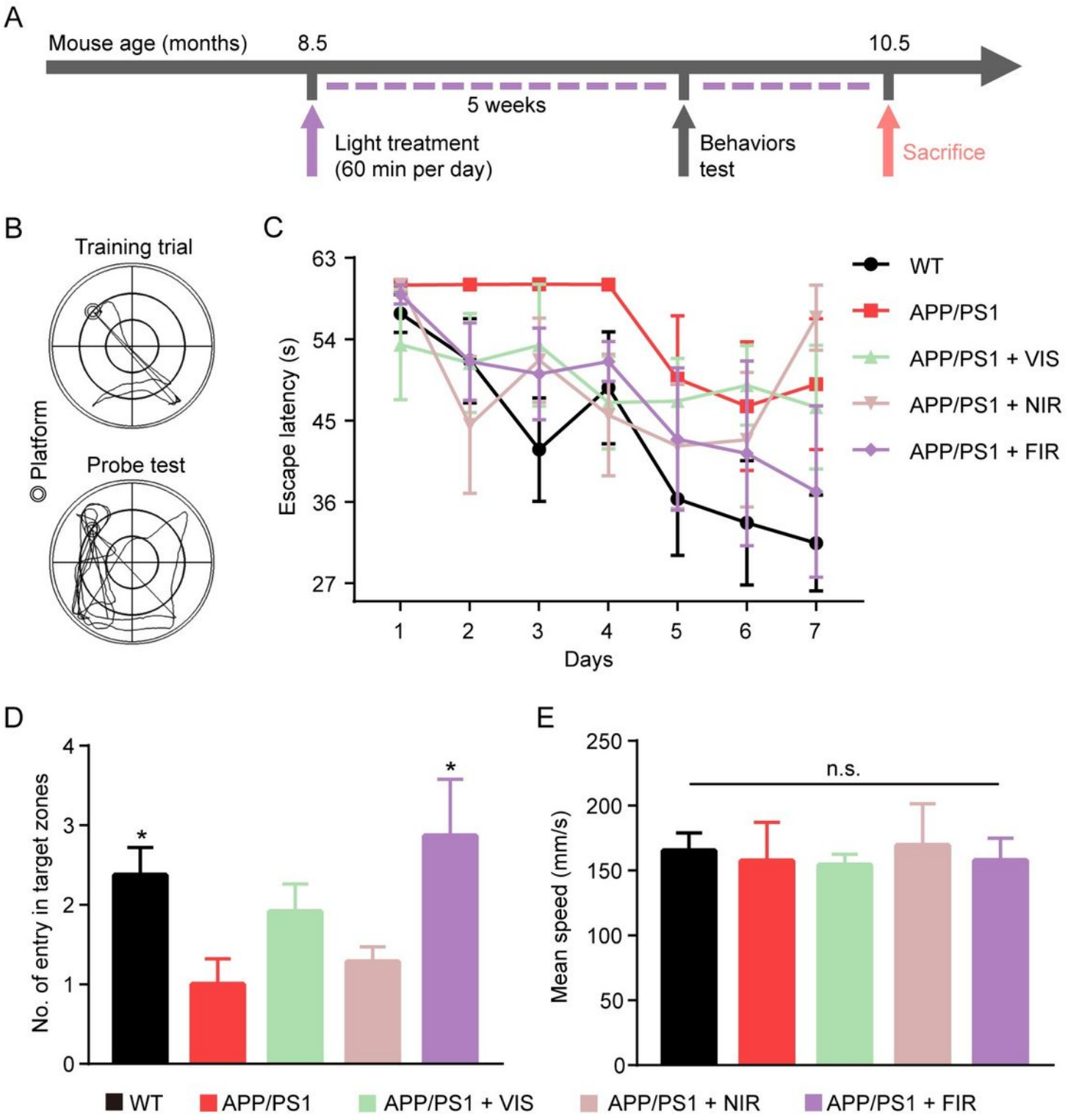

Figure 1

FIR light ameliorated learning and memory deficit of AD-like mice. (A) Timeline of treatment with visible light (VIS), near infrared light (NIR) and far infrared light (FIR) on APP/PS1 mice. (B) Representative tracking routes of mice in training trials and spatial probe test. (C) The escape latency of mice to find the platform during training trials. (D) The number of entries in the zones around platform. (E) The mean

swimming speed of mice. Data were means ± S.E.M. (n = 5 - 8). *p < 0.05 compared to APP/PS1 mice without light treatment.

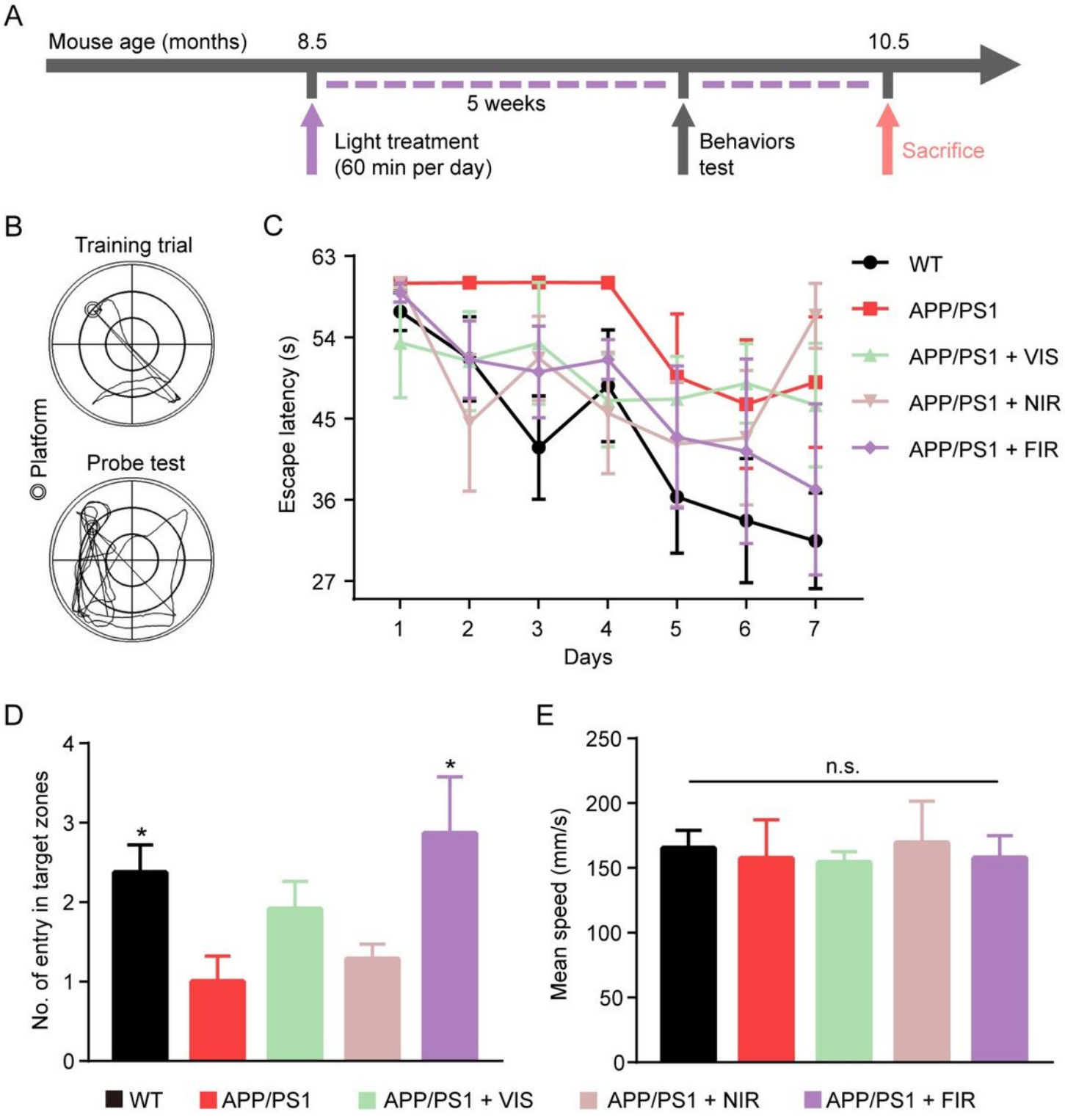

Figure 1

FIR light ameliorated learning and memory deficit of AD-like mice. (A) Timeline of treatment with visible light (VIS), near infrared light (NIR) and far infrared light (FIR) on APP/PS1 mice. (B) Representative tracking routes of mice in training trials and spatial probe test. (C) The escape latency of mice to find the

platform during training trials. (D) The number of entries in the zones around platform. (E) The mean swimming speed of mice. Data were means ± S.E.M. (n = 5 - 8). *p < 0.05 compared to APP/PS1 mice without light treatment.

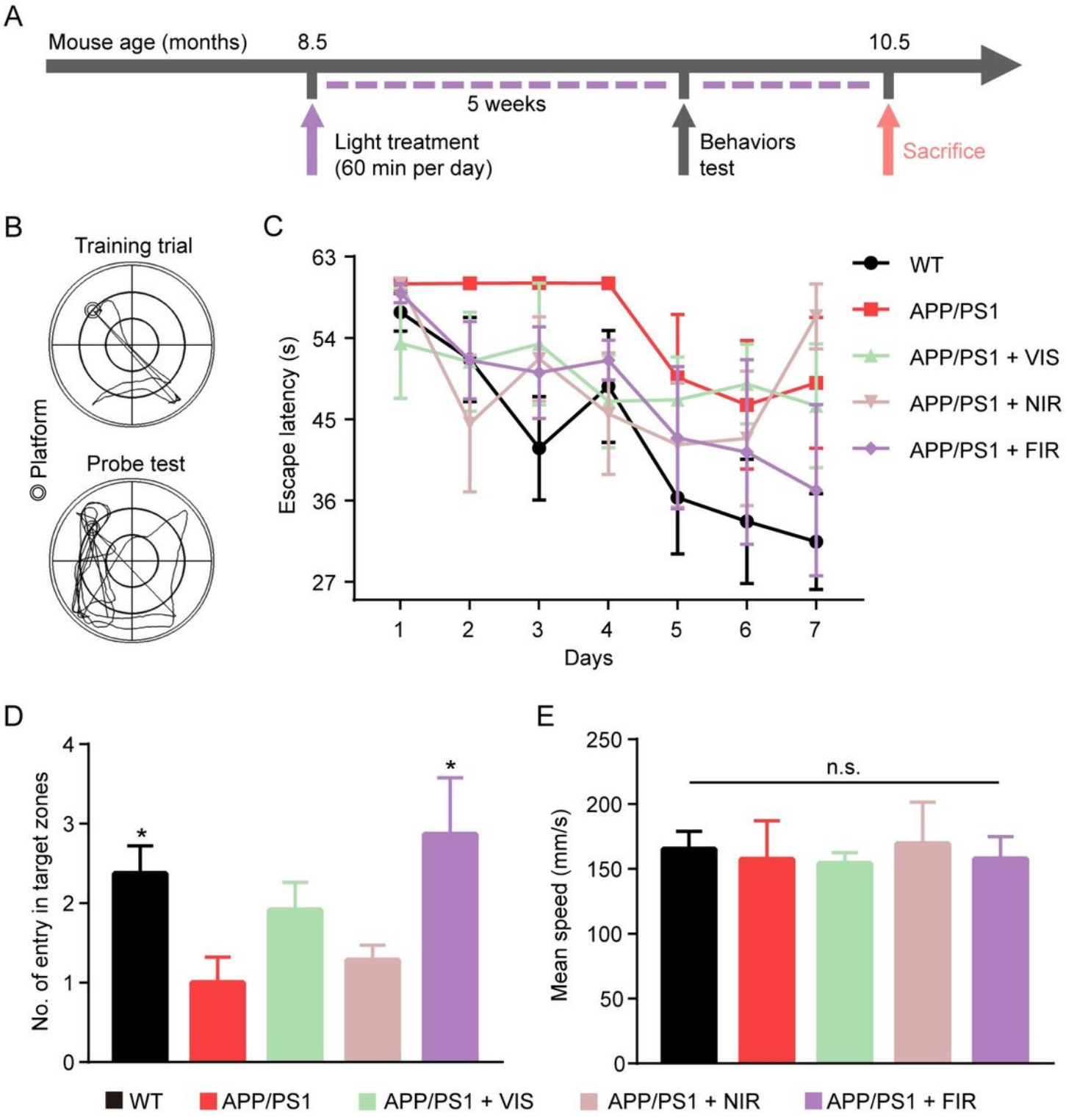

Figure 1

FIR light ameliorated learning and memory deficit of AD-like mice. (A) Timeline of treatment with visible light (VIS), near infrared light (NIR) and far infrared light (FIR) on APP/PS1 mice. (B) Representative

tracking routes of mice in training trials and spatial probe test. (C) The escape latency of mice to find the platform during training trials. (D) The number of entries in the zones around platform. (E) The mean swimming speed of mice. Data were means ± S.E.M. (n = 5 - 8). *p < 0.05 compared to APP/PS1 mice without light treatment.

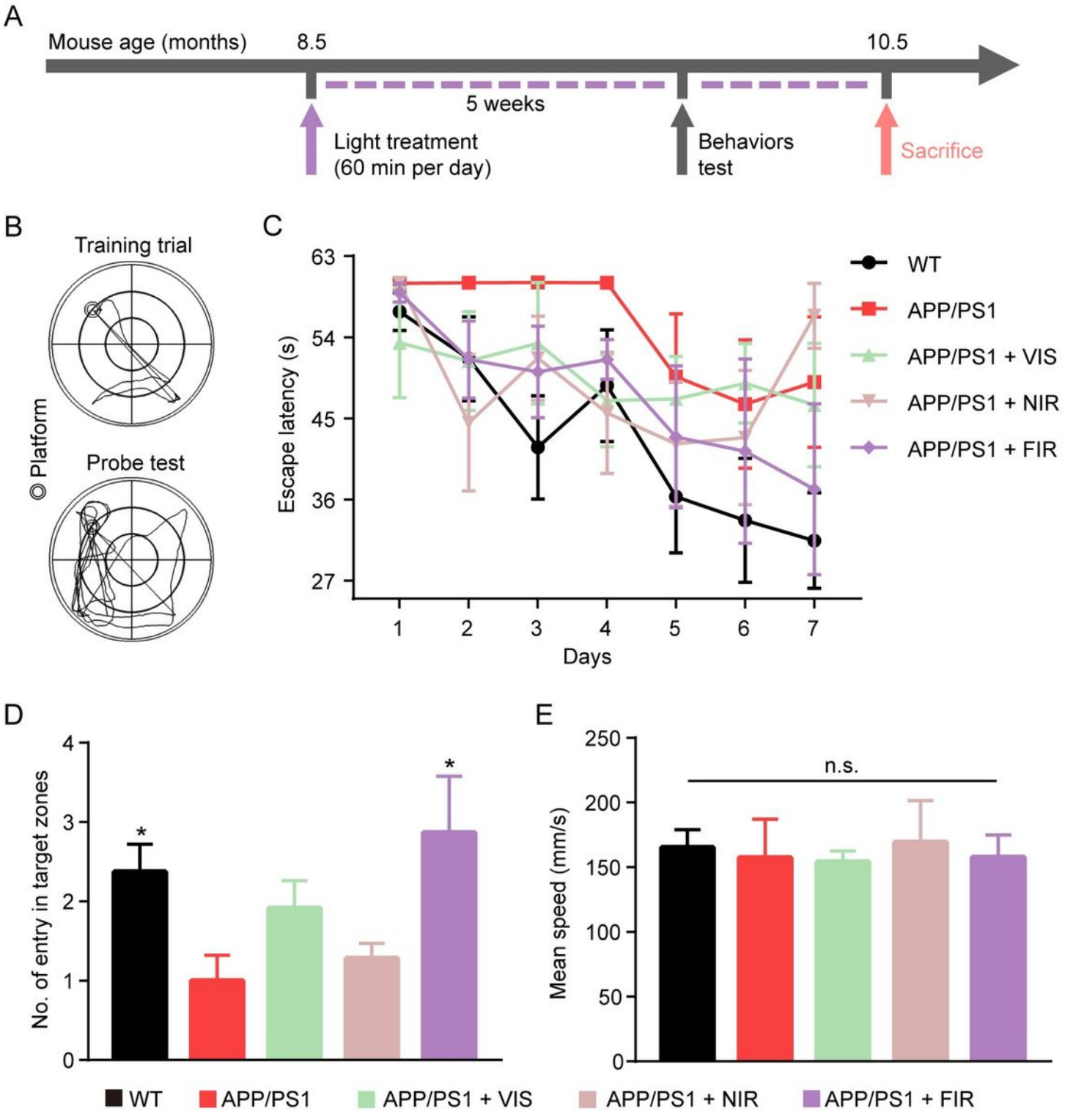

Figure 1

FIR light ameliorated learning and memory deficit of AD-like mice. (A) Timeline of treatment with visible light (VIS), near infrared light (NIR) and far infrared light (FIR) on APP/PS1 mice. (B) Representative tracking routes of mice in training trials and spatial probe test. (C) The escape latency of mice to find the platform during training trials. (D) The number of entries in the zones around platform. (E) The mean swimming speed of mice. Data were means ± S.E.M. (n = 5 - 8). *p < 0.05 compared to APP/PS1 mice without light treatment.

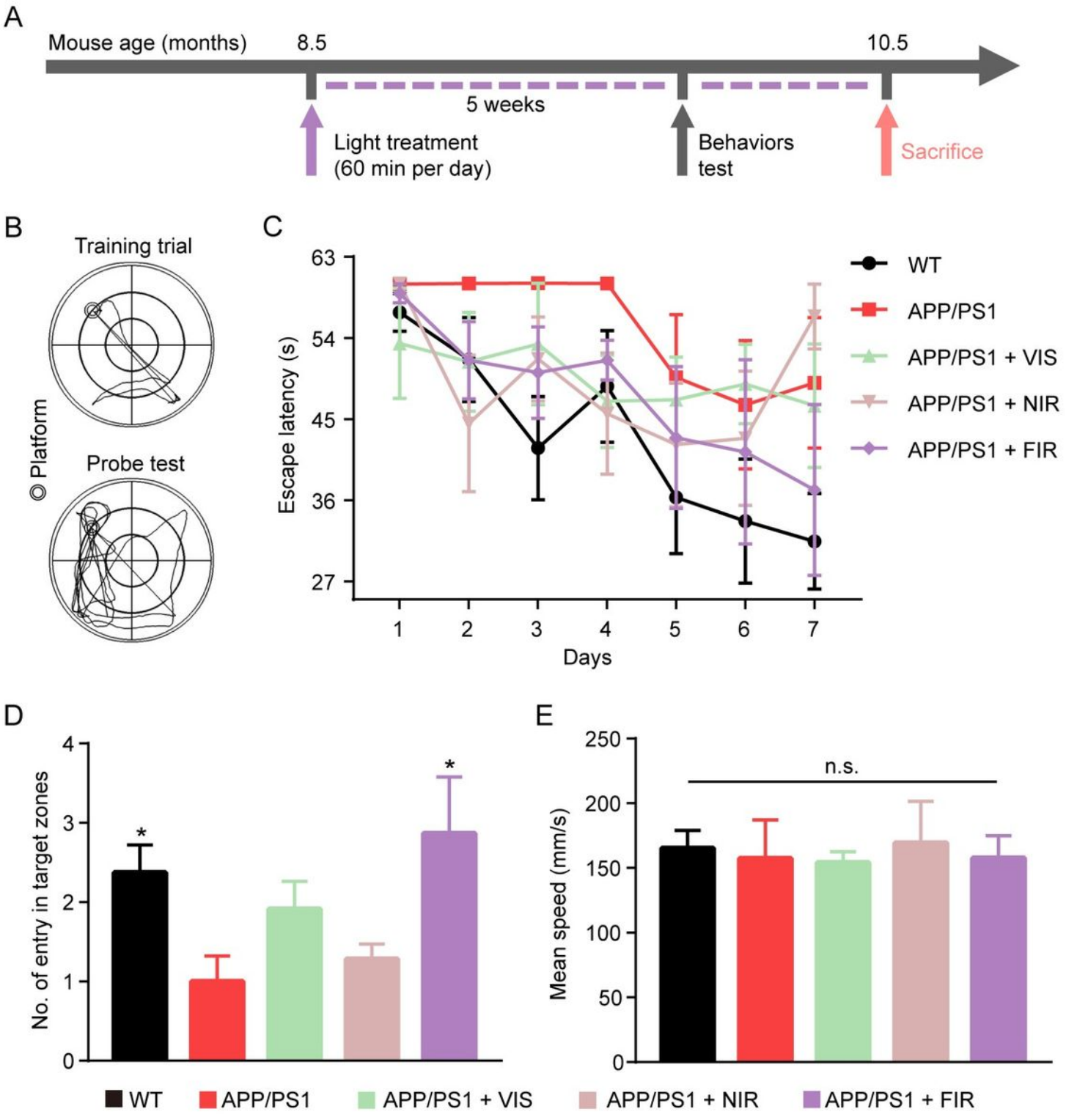

Figure 1

FIR light ameliorated learning and memory deficit of AD-like mice. (A) Timeline of treatment with visible light (VIS), near infrared light (NIR) and far infrared light (FIR) on APP/PS1 mice. (B) Representative tracking routes of mice in training trials and spatial probe test. (C) The escape latency of mice to find the platform during training trials. (D) The number of entries in the zones around platform. (E) The mean swimming speed of mice. Data were means ± S.E.M. (n = 5 - 8). *p < 0.05 compared to APP/PS1 mice without light treatment.

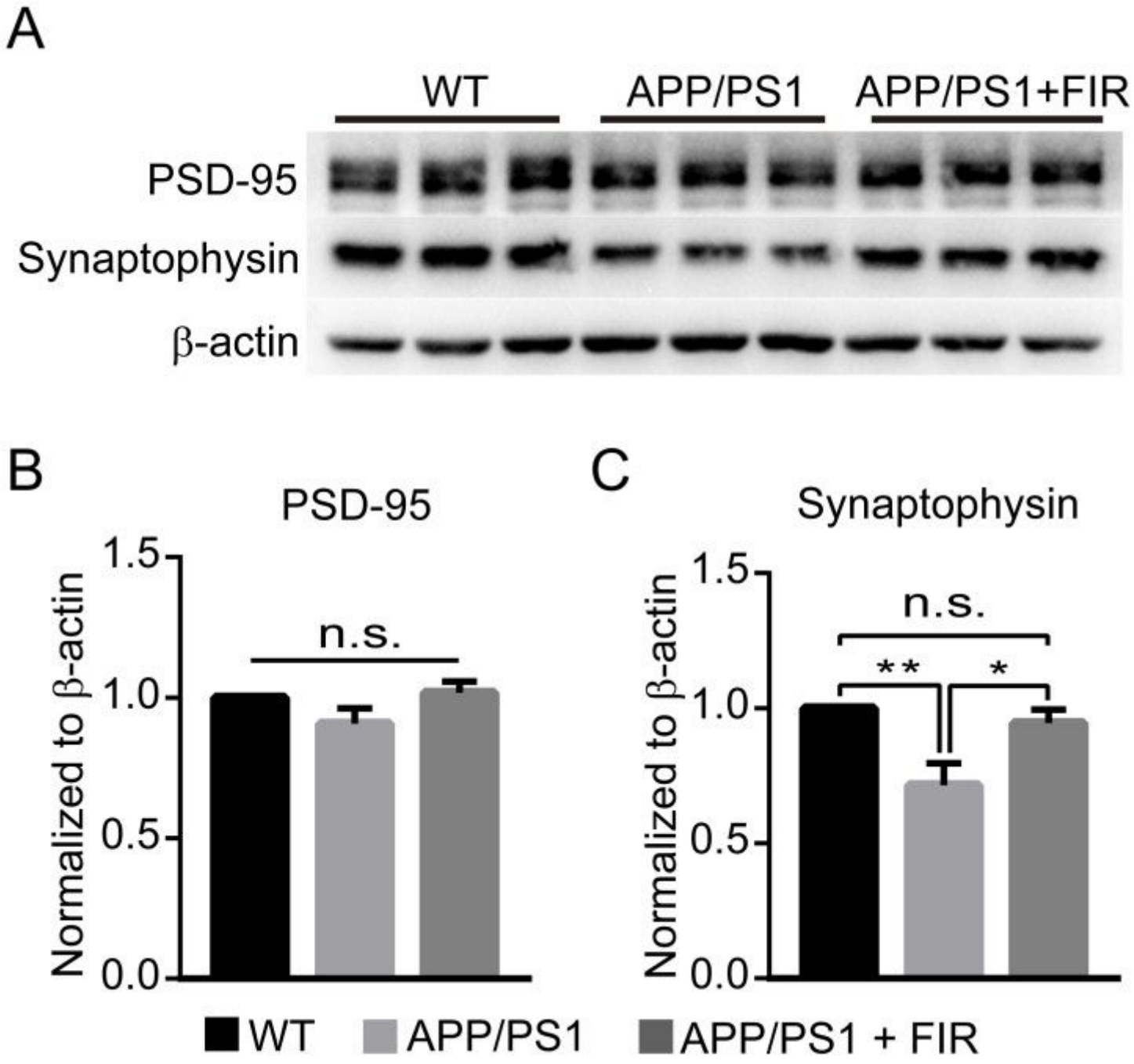

Figure 2

FIR light treatment restored the expression of synaptic protein in AD-like mice. (A) Representative images of Western blotting. (B) Quantification of PSD-95. (C) Quantification of synaptophysin. Data were means

± S.E.M. (n = 5), *p < 0.05 and **p < 0.01 compared to APP/PS1 mice without FIR light treatment.

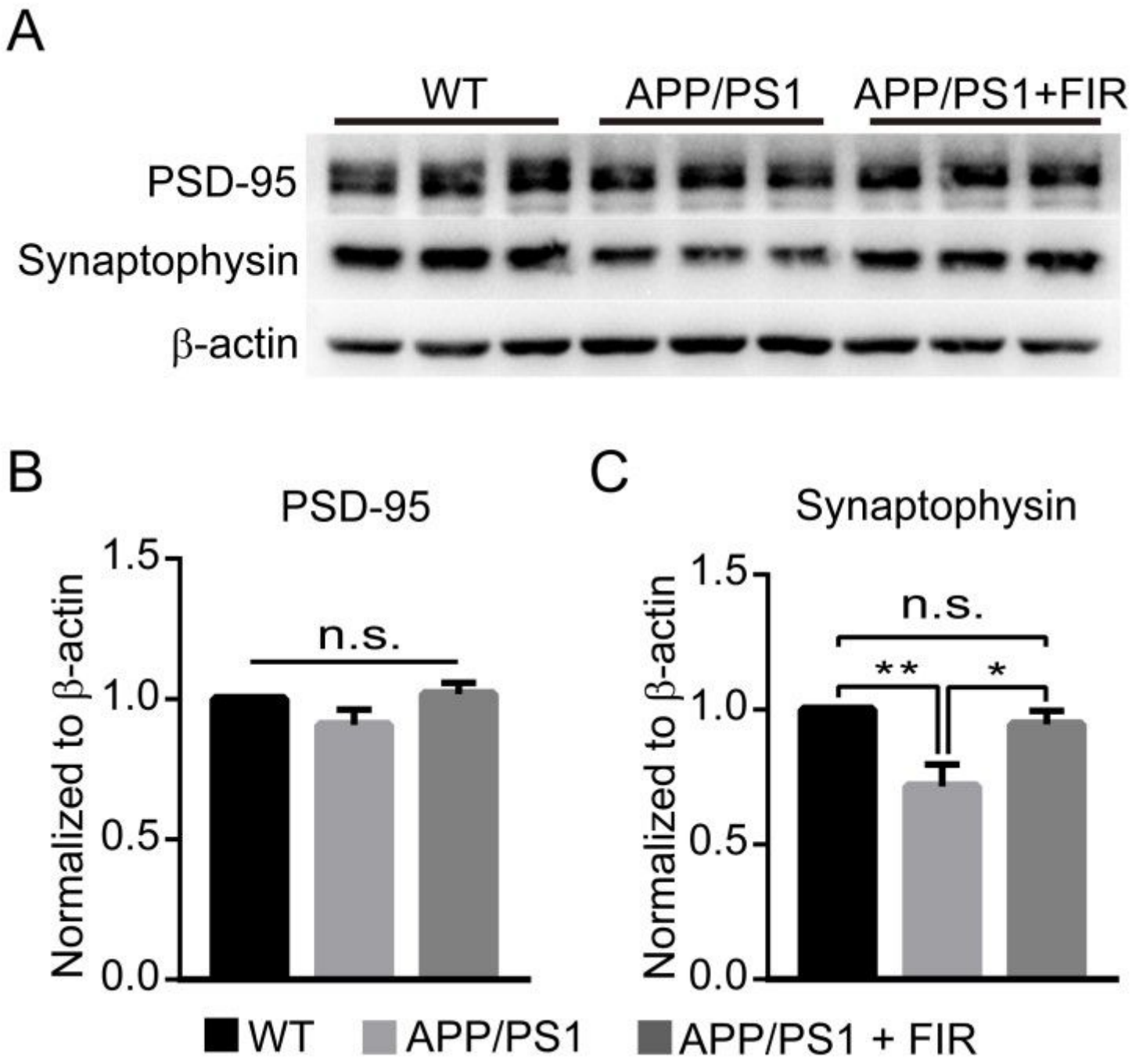

Figure 2

FIR light treatment restored the expression of synaptic protein in AD-like mice. (A) Representative images of Western blotting. (B) Quantification of PSD-95. (C) Quantification of synaptophysin. Data were means ± S.E.M. (n = 5), *p < 0.05 and **p < 0.01 compared to APP/PS1 mice without FIR light treatment.

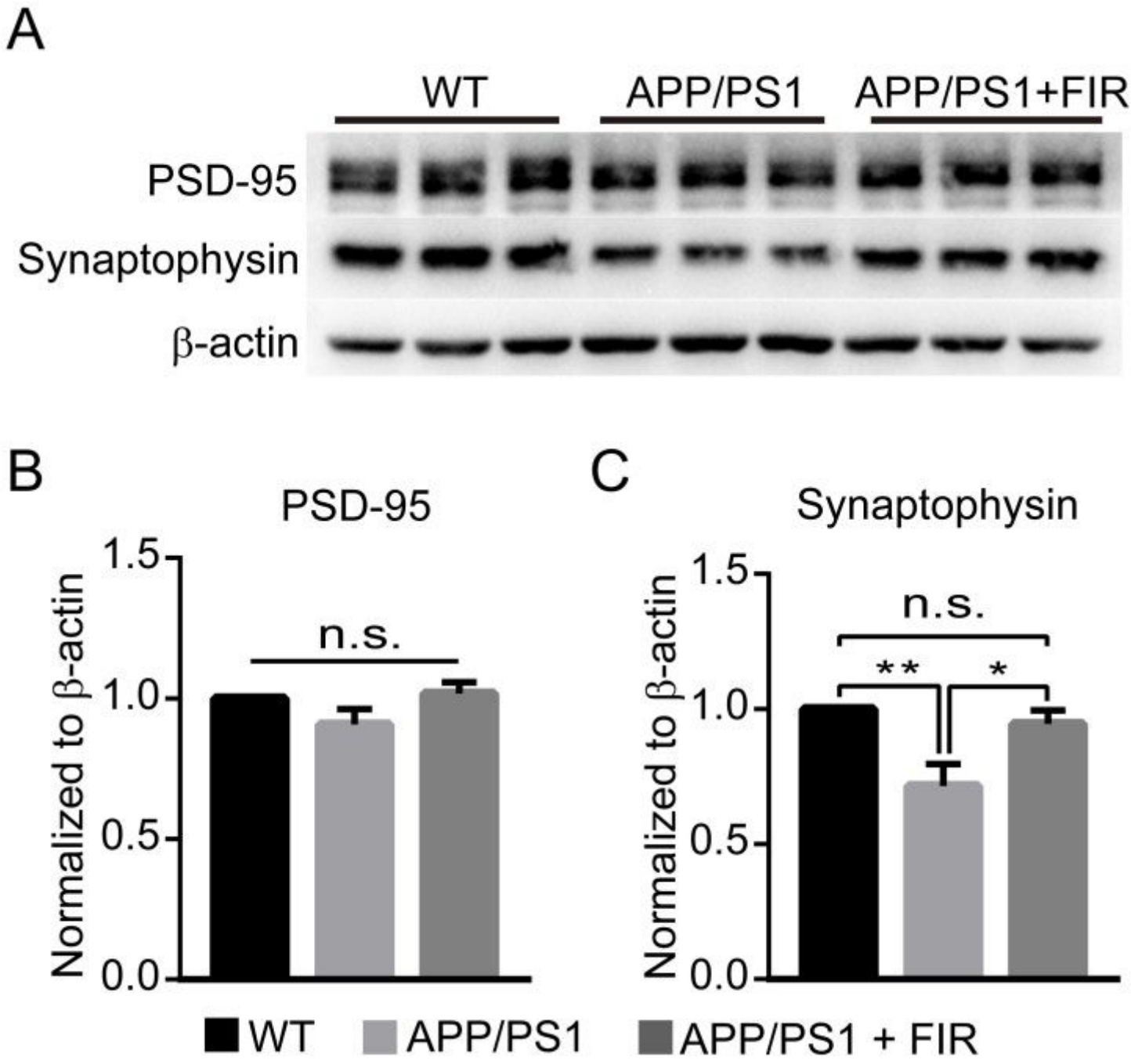

Figure 2

FIR light treatment restored the expression of synaptic protein in AD-like mice. (A) Representative images of Western blotting. (B) Quantification of PSD-95. (C) Quantification of synaptophysin. Data were means ± S.E.M. (n = 5), *p < 0.05 and **p < 0.01 compared to APP/PS1 mice without FIR light treatment.

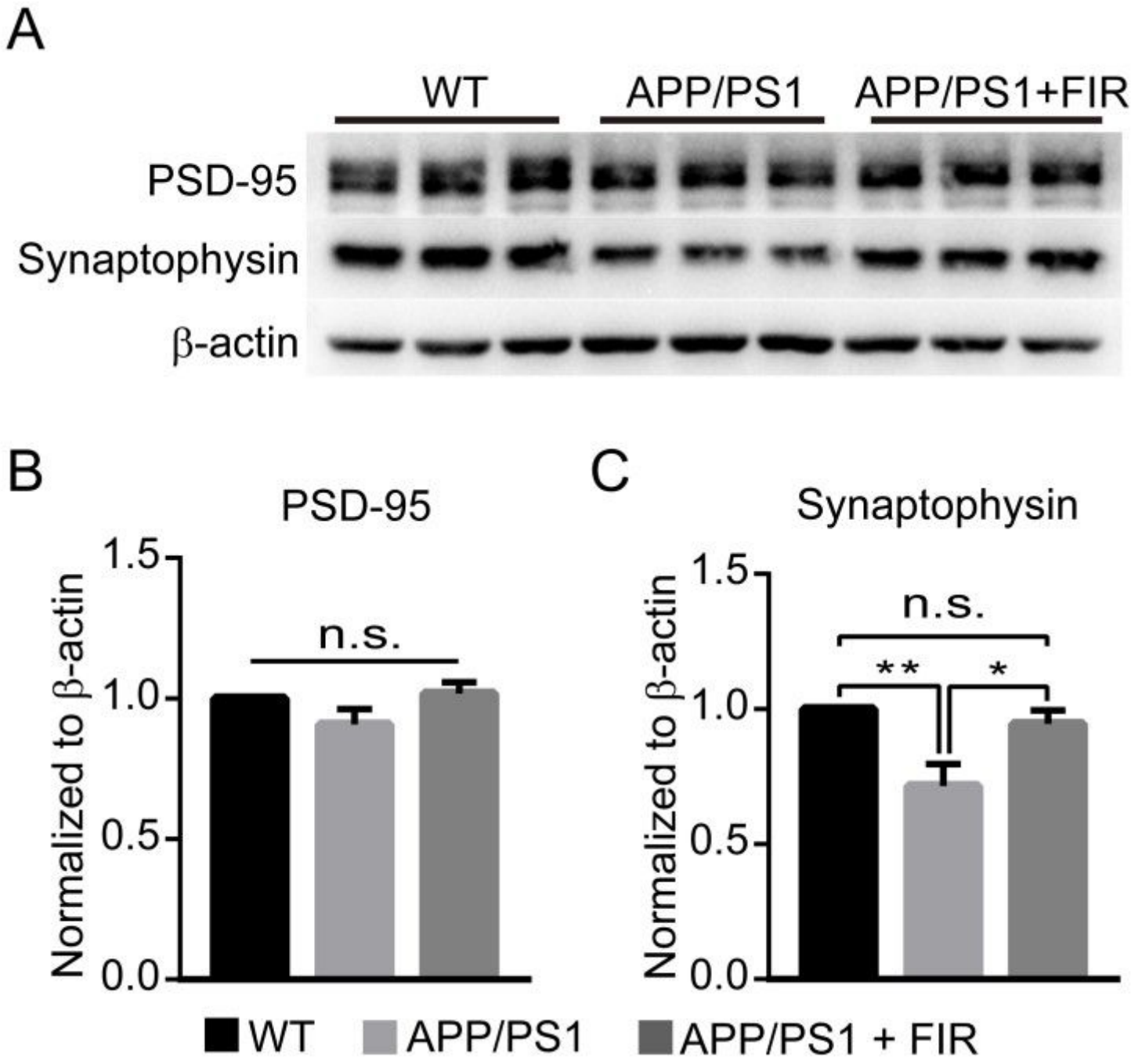

Figure 2

FIR light treatment restored the expression of synaptic protein in AD-like mice. (A) Representative images of Western blotting. (B) Quantification of PSD-95. (C) Quantification of synaptophysin. Data were means ± S.E.M. (n = 5), *p < 0.05 and **p < 0.01 compared to APP/PS1 mice without FIR light treatment.

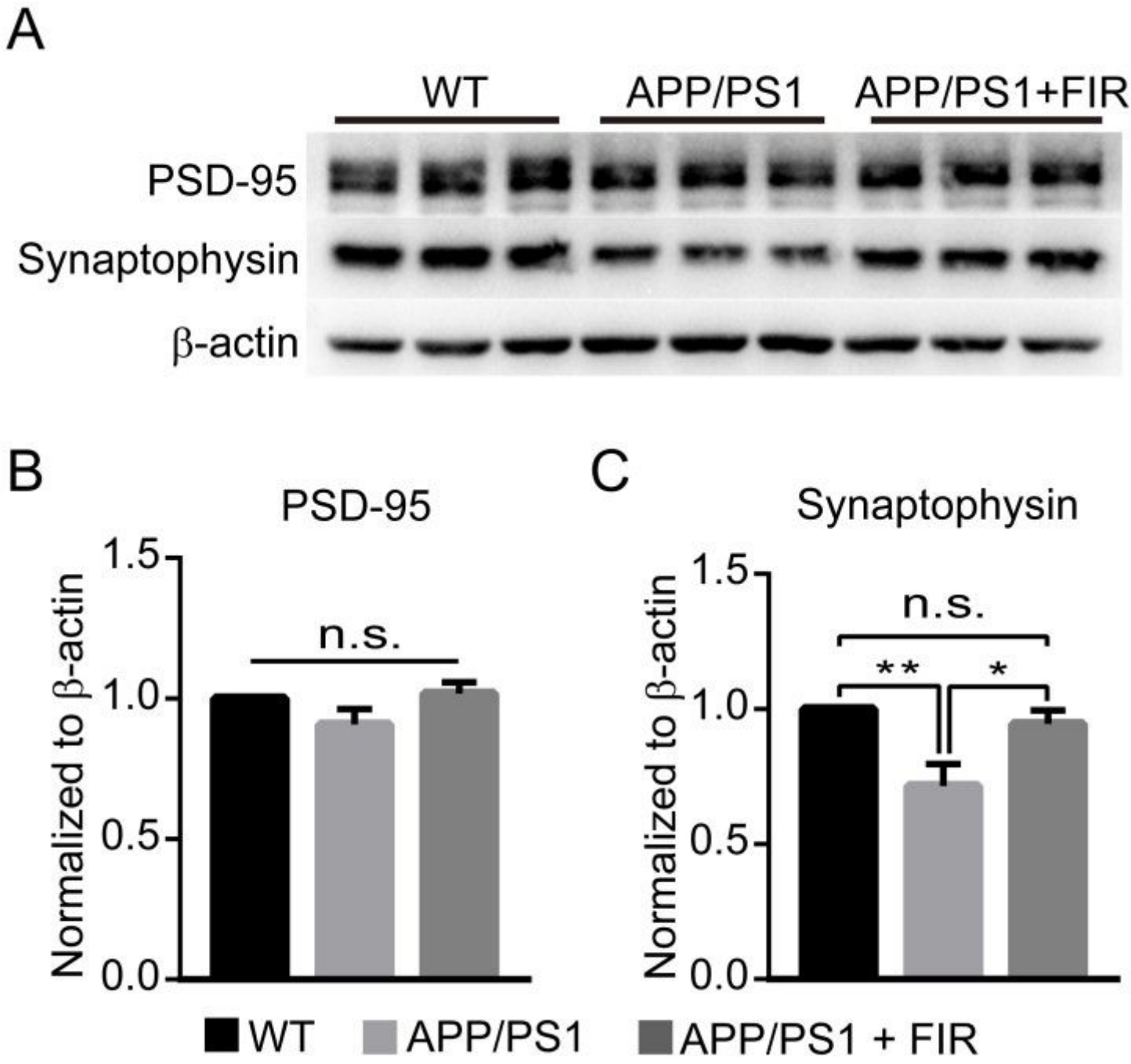

Figure 2

FIR light treatment restored the expression of synaptic protein in AD-like mice. (A) Representative images of Western blotting. (B) Quantification of PSD-95. (C) Quantification of synaptophysin. Data were means ± S.E.M. (n = 5), *p < 0.05 and **p < 0.01 compared to APP/PS1 mice without FIR light treatment.

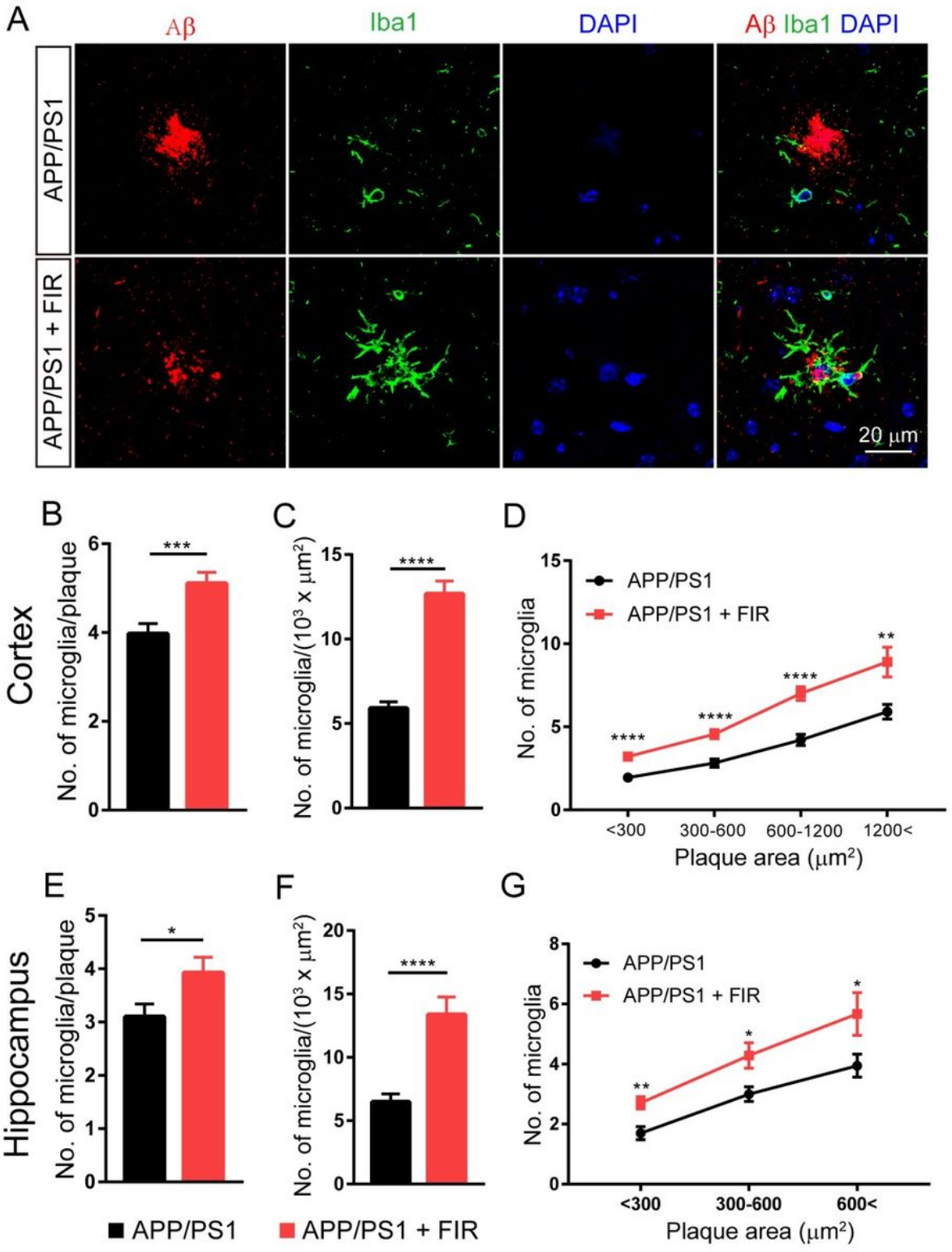

Figure 3

FIR light promoted microglial recruitment to Aβ plaques. (A) Representative images of Aβ (6E10, red), microglia (Iba1, green) and nuclei (DAPI, blue) co-staining from APP/PS1 treated with or without FIR light. (B) Quantification of microglial cells within 20 μm from the Aβ plaque boundary (n = 102 to 103 plaques per group) in the cerebral cortex. (C) Quantification of microglial cells normalized to Aβ plaque area (103 μm2) in the cerebral cortex. (D) Quantification of microglia per plaque of different sizes in the cerebral

cortex. (E) Quantification of microglial cells within 20 μm from the Aβ plaque boundary (n = 40 plaques per group) in the hippocampus. (F) Quantification of microglial cells normalized to Aβ plaque area (103 μm2) in the hippocampus (G) Quantification of microglia per plaque of different sizes in the hippocampus. Data are means ± S.E.M. *P < 0.05, **P < 0.01, ***P < 0.001 and ****P < 0.0001 compared to corresponding values of APP/PS1 mice without FIR light treatment.

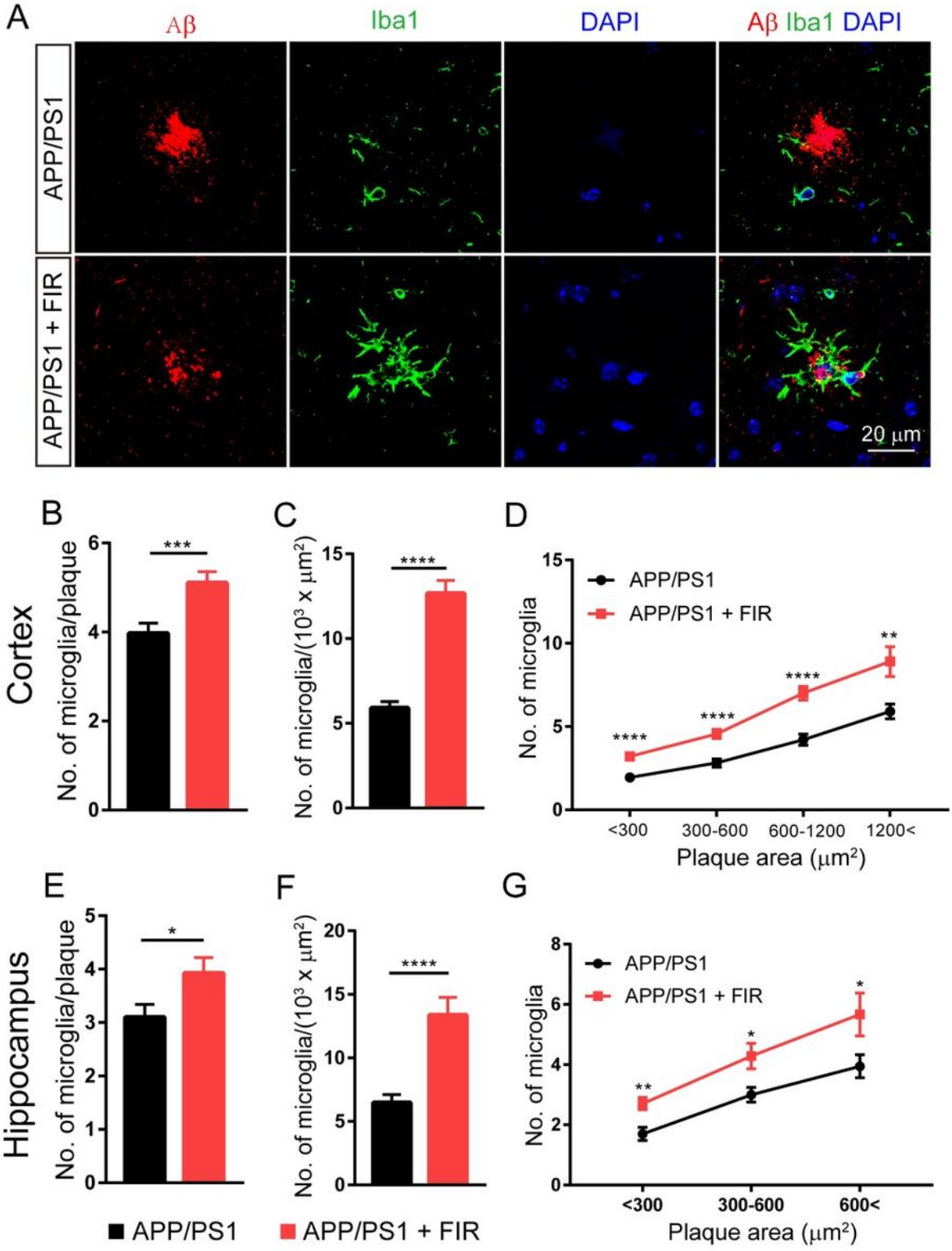

Figure 3

FIR light promoted microglial recruitment to Aβ plaques. (A) Representative images of Aβ (6E10, red), microglia (Iba1, green) and nuclei (DAPI, blue) co-staining from APP/PS1 treated with or without FIR light. (B) Quantification of microglial cells within 20 μm from the Aβ plaque boundary (n = 102 to 103 plaques per group) in the cerebral cortex. (C) Quantification of microglial cells normalized to Aβ plaque area (103 μm2) in the cerebral cortex. (D) Quantification of microglia per plaque of different sizes in the cerebral cortex. (E) Quantification of microglial cells within 20 μm from the Aβ plaque boundary (n = 40 plaques per group) in the hippocampus. (F) Quantification of microglial cells normalized to Aβ plaque area (103 μm2) in the hippocampus (G) Quantification of microglia per plaque of different sizes in the hippocampus. Data are means ± S.E.M. *P < 0.05, **P < 0.01, ***P < 0.001 and ****P < 0.0001 compared to corresponding values of APP/PS1 mice without FIR light treatment.

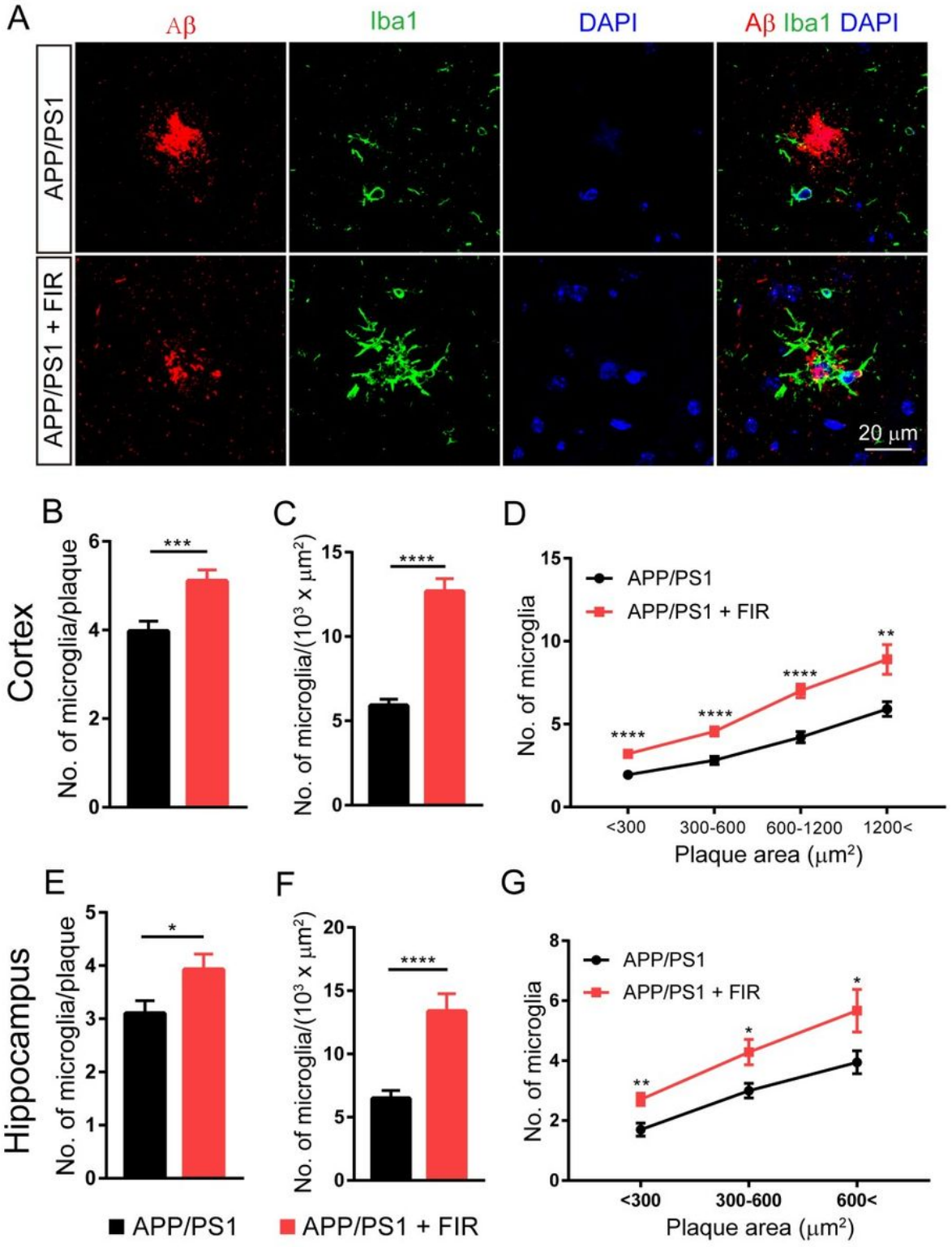

Figure 3

FIR light promoted microglial recruitment to Aβ plaques. (A) Representative images of Aβ (6E10, red), microglia (Iba1, green) and nuclei (DAPI, blue) co-staining from APP/PS1 treated with or without FIR light. (B) Quantification of microglial cells within 20 μm from the Aβ plaque boundary (n = 102 to 103 plaques per group) in the cerebral cortex. (C) Quantification of microglial cells normalized to Aβ plaque area (103 μm2) in the cerebral cortex. (D) Quantification of microglia per plaque of different sizes in the cerebral

cortex. (E) Quantification of microglial cells within 20 μm from the Aβ plaque boundary (n = 40 plaques per group) in the hippocampus. (F) Quantification of microglial cells normalized to Aβ plaque area (103 μm2) in the hippocampus (G) Quantification of microglia per plaque of different sizes in the hippocampus. Data are means ± S.E.M. *P < 0.05, **P < 0.01, ***P < 0.001 and ****P < 0.0001 compared to corresponding values of APP/PS1 mice without FIR light treatment.

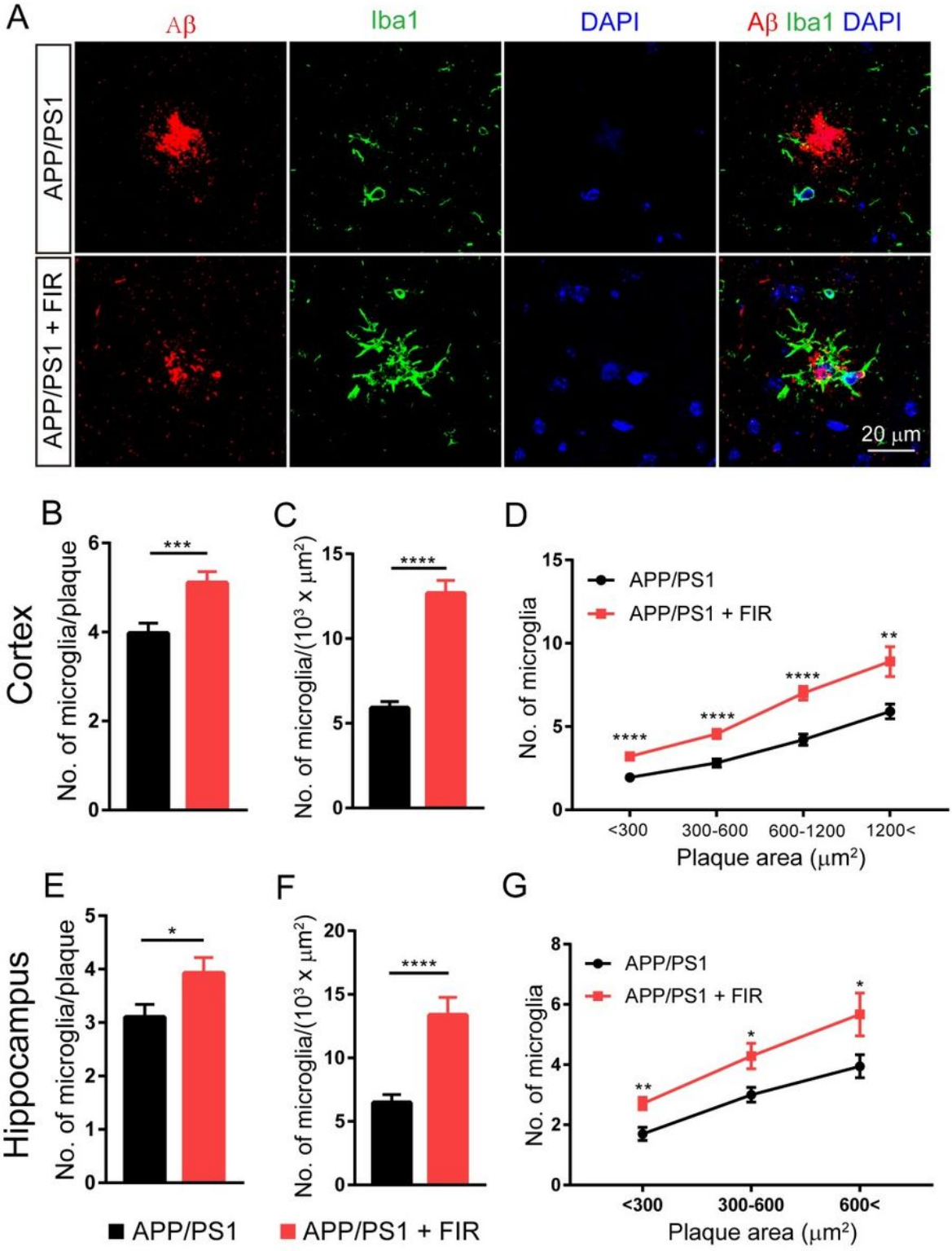

Figure 3

FIR light promoted microglial recruitment to Aβ plaques. (A) Representative images of Aβ (6E10, red), microglia (Iba1, green) and nuclei (DAPI, blue) co-staining from APP/PS1 treated with or without FIR light. (B) Quantification of microglial cells within 20 μm from the Aβ plaque boundary (n = 102 to 103 plaques per group) in the cerebral cortex. (C) Quantification of microglial cells normalized to Aβ plaque area (103 μm2) in the cerebral cortex. (D) Quantification of microglia per plaque of different sizes in the cerebral cortex. (E) Quantification of microglial cells within 20 μm from the Aβ plaque boundary (n = 40 plaques per group) in the hippocampus. (F) Quantification of microglial cells normalized to Aβ plaque area (103 μm2) in the hippocampus (G) Quantification of microglia per plaque of different sizes in the hippocampus. Data are means ± S.E.M. *P < 0.05, **P < 0.01, ***P < 0.001 and ****P < 0.0001 compared to corresponding values of APP/PS1 mice without FIR light treatment.

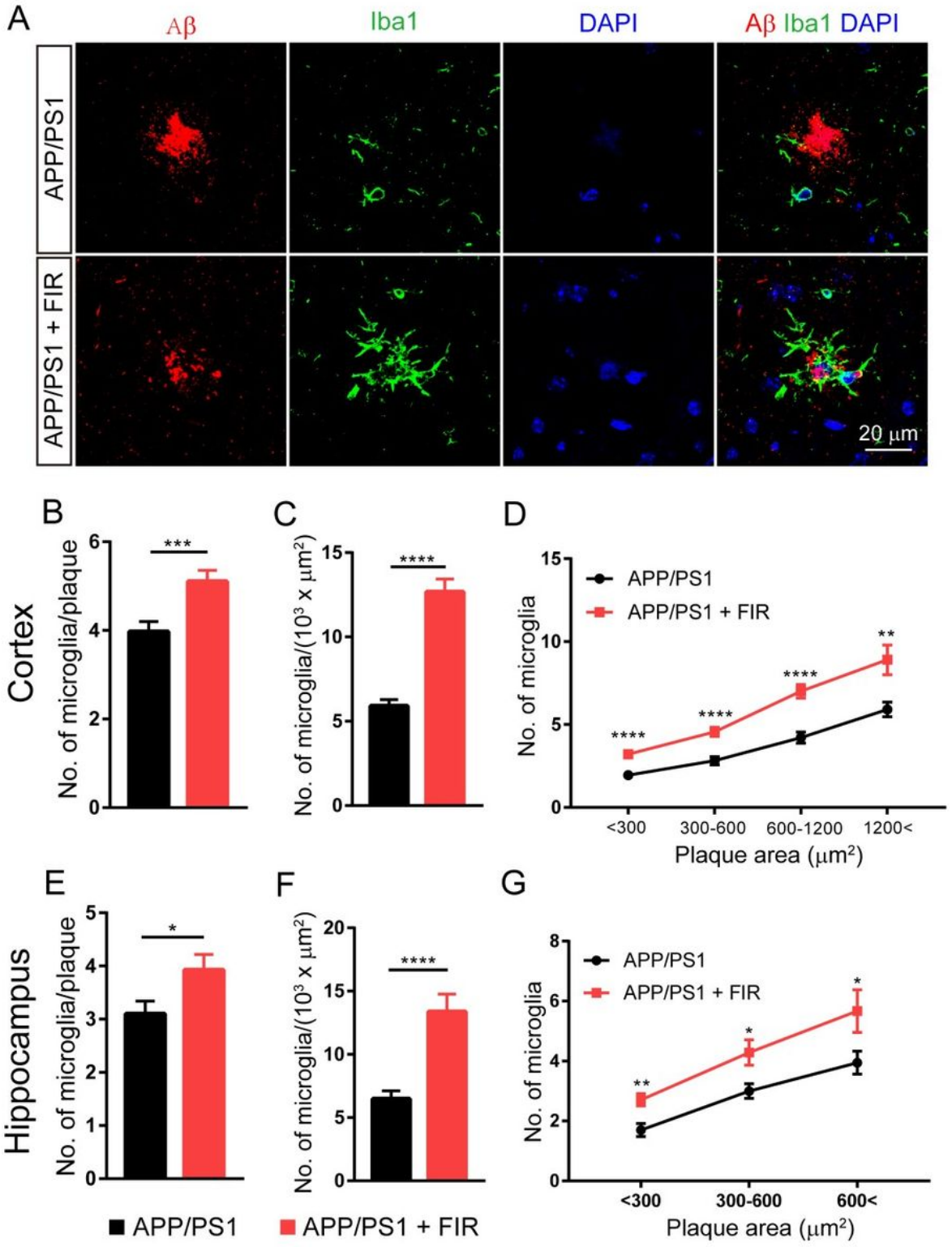

Figure 3

FIR light promoted microglial recruitment to Aβ plaques. (A) Representative images of Aβ (6E10, red), microglia (Iba1, green) and nuclei (DAPI, blue) co-staining from APP/PS1 treated with or without FIR light. (B) Quantification of microglial cells within 20 μm from the Aβ plaque boundary (n = 102 to 103 plaques per group) in the cerebral cortex. (C) Quantification of microglial cells normalized to Aβ plaque area (103 μm2) in the cerebral cortex. (D) Quantification of microglia per plaque of different sizes in the cerebral

cortex. (E) Quantification of microglial cells within 20 μm from the Aβ plaque boundary (n = 40 plaques per group) in the hippocampus. (F) Quantification of microglial cells normalized to Aβ plaque area (103 μm2) in the hippocampus (G) Quantification of microglia per plaque of different sizes in the hippocampus. Data are means ± S.E.M. *P < 0.05, **P < 0.01, ***P < 0.001 and ****P < 0.0001 compared to corresponding values of APP/PS1 mice without FIR light treatment.

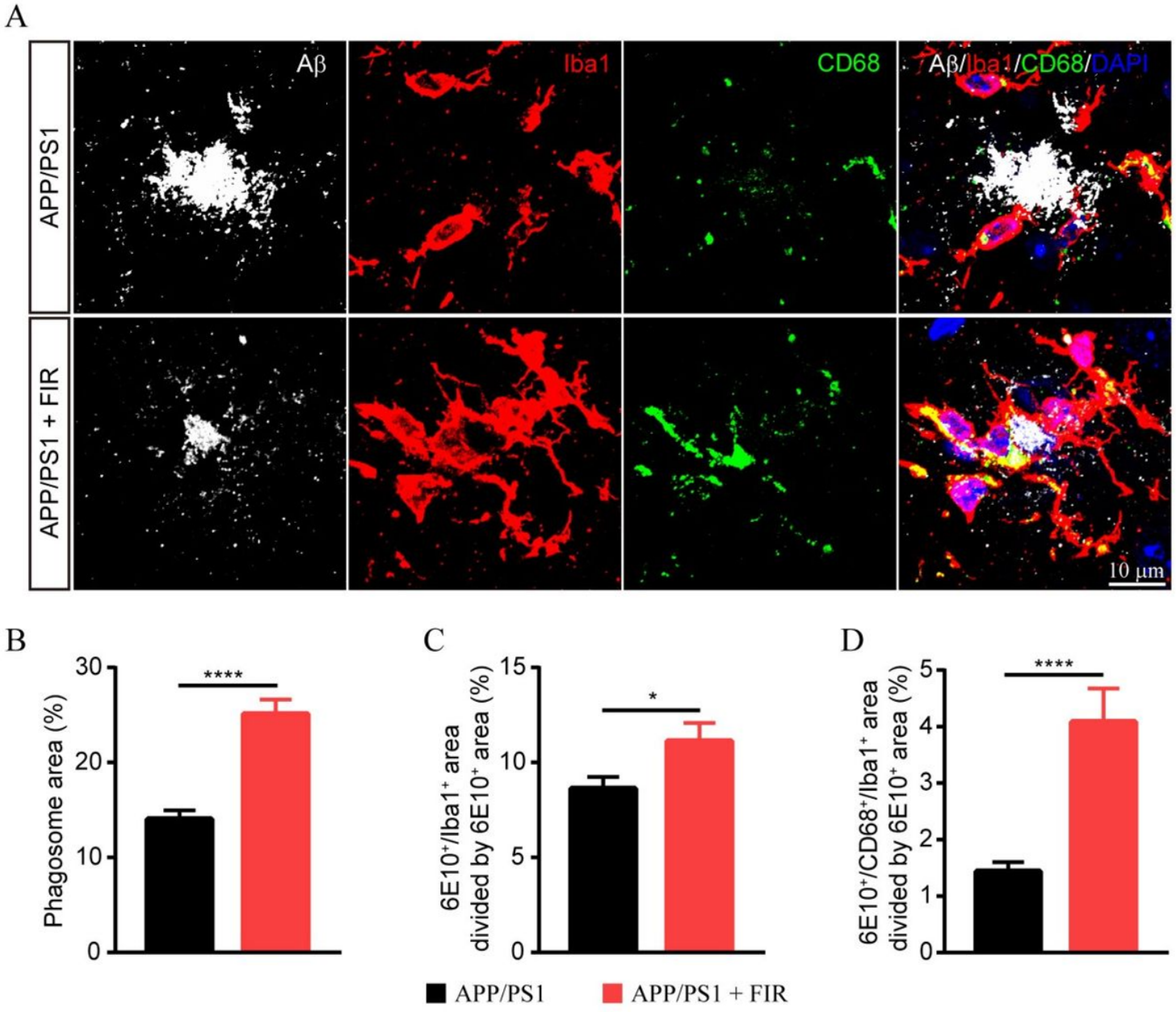

Figure 4

FIR light enhanced microglial phagocytosis of Aβ under in vivo condition. (A) Representative images of Aβ (6E10, white), microglia (Iba1, red), phagosome (CD68, green) and nuclei (DAPI, blue) co-staining in the cerebral cortex of APP/PS1 mice treated with or without FIR light. (B) Quantification of the percentage of phagosome area in Iba1 positive area. (C) Quantification of the percentage of 6E10+/Iba1+ co-staining area normalized to the total 6E10+ area. (D) Quantification of the percentage of 6E10+/CD68+/Iba1+ co-

staining area normalized to the total 6E10+ area. Data were means ± S.E.M. (n = 49 - 52 per group). *P < 0.05 and ****P < 0.0001 compared to corresponding values of APP/PS1 mice without FIR light treatment.

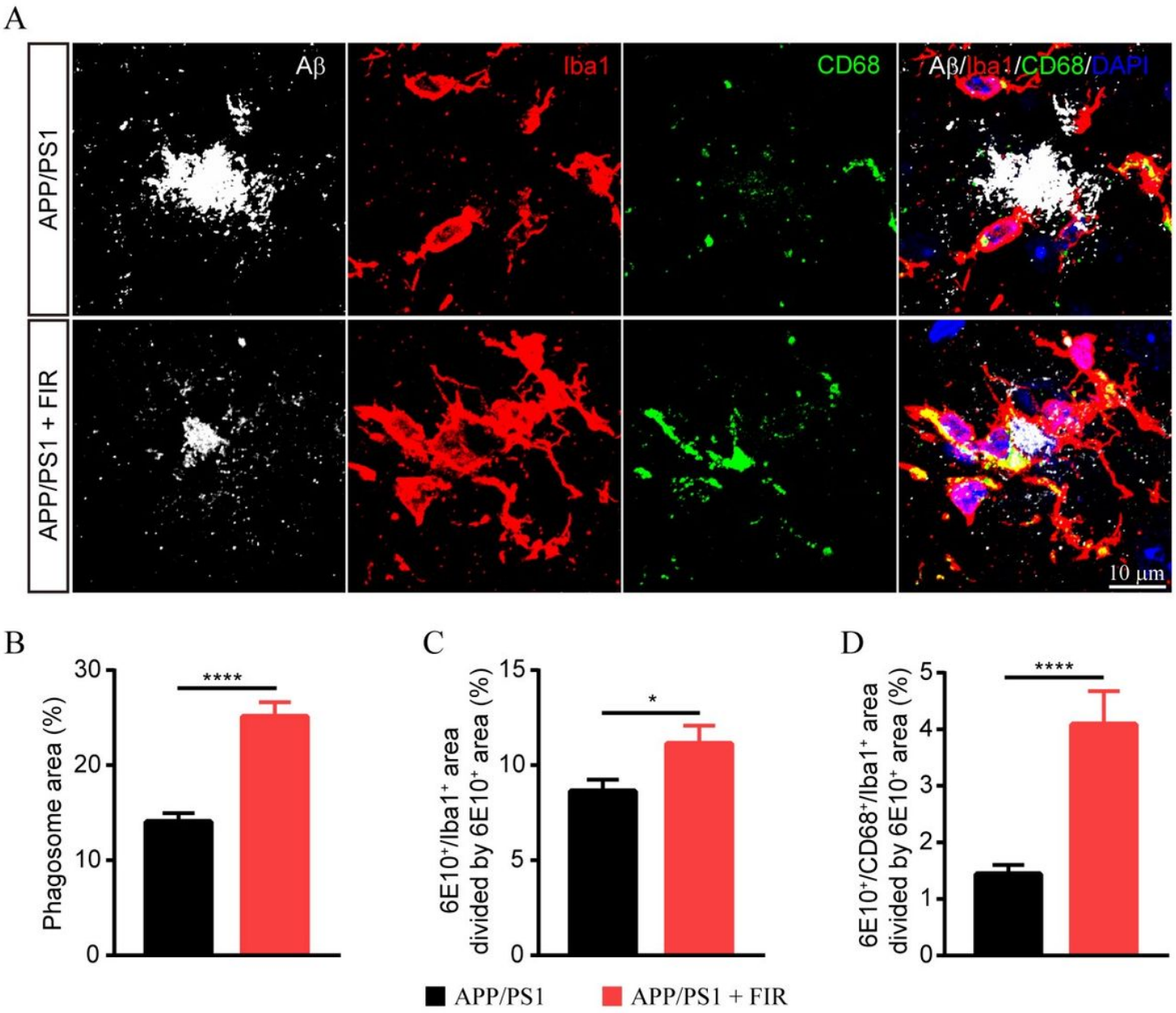

Figure 4

FIR light enhanced microglial phagocytosis of Aβ under in vivo condition. (A) Representative images of Aβ (6E10, white), microglia (Iba1, red), phagosome (CD68, green) and nuclei (DAPI, blue) co-staining in the cerebral cortex of APP/PS1 mice treated with or without FIR light. (B) Quantification of the percentage of phagosome area in Iba1 positive area. (C) Quantification of the percentage of 6E10+/Iba1+ co-staining area normalized to the total 6E10+ area. (D) Quantification of the percentage of 6E10+/CD68+/Iba1+ co-staining area normalized to the total 6E10+ area. Data were means ± S.E.M. (n = 49 - 52 per group). *P < 0.05 and ****P < 0.0001 compared to corresponding values of APP/PS1 mice without FIR light treatment.

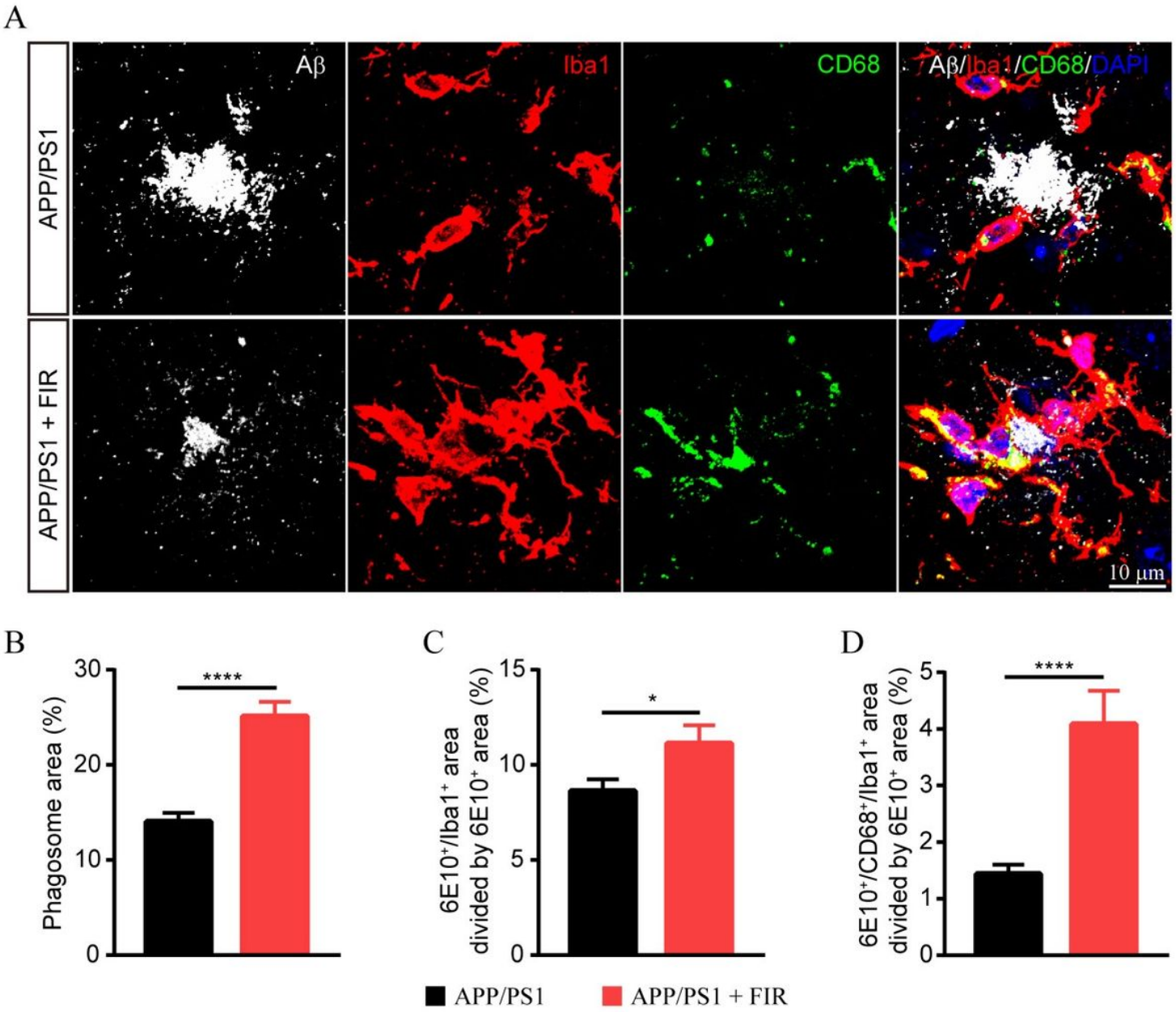

Figure 4

FIR light enhanced microglial phagocytosis of Aβ under in vivo condition. (A) Representative images of Aβ (6E10, white), microglia (Iba1, red), phagosome (CD68, green) and nuclei (DAPI, blue) co-staining in the cerebral cortex of APP/PS1 mice treated with or without FIR light. (B) Quantification of the percentage of phagosome area in Iba1 positive area. (C) Quantification of the percentage of 6E10+/Iba1+ co-staining area normalized to the total 6E10+ area. (D) Quantification of the percentage of 6E10+/CD68+/Iba1+ co-staining area normalized to the total 6E10+ area. Data were means ± S.E.M. (n = 49 - 52 per group). *P < 0.05 and ****P < 0.0001 compared to corresponding values of APP/PS1 mice without FIR light treatment.

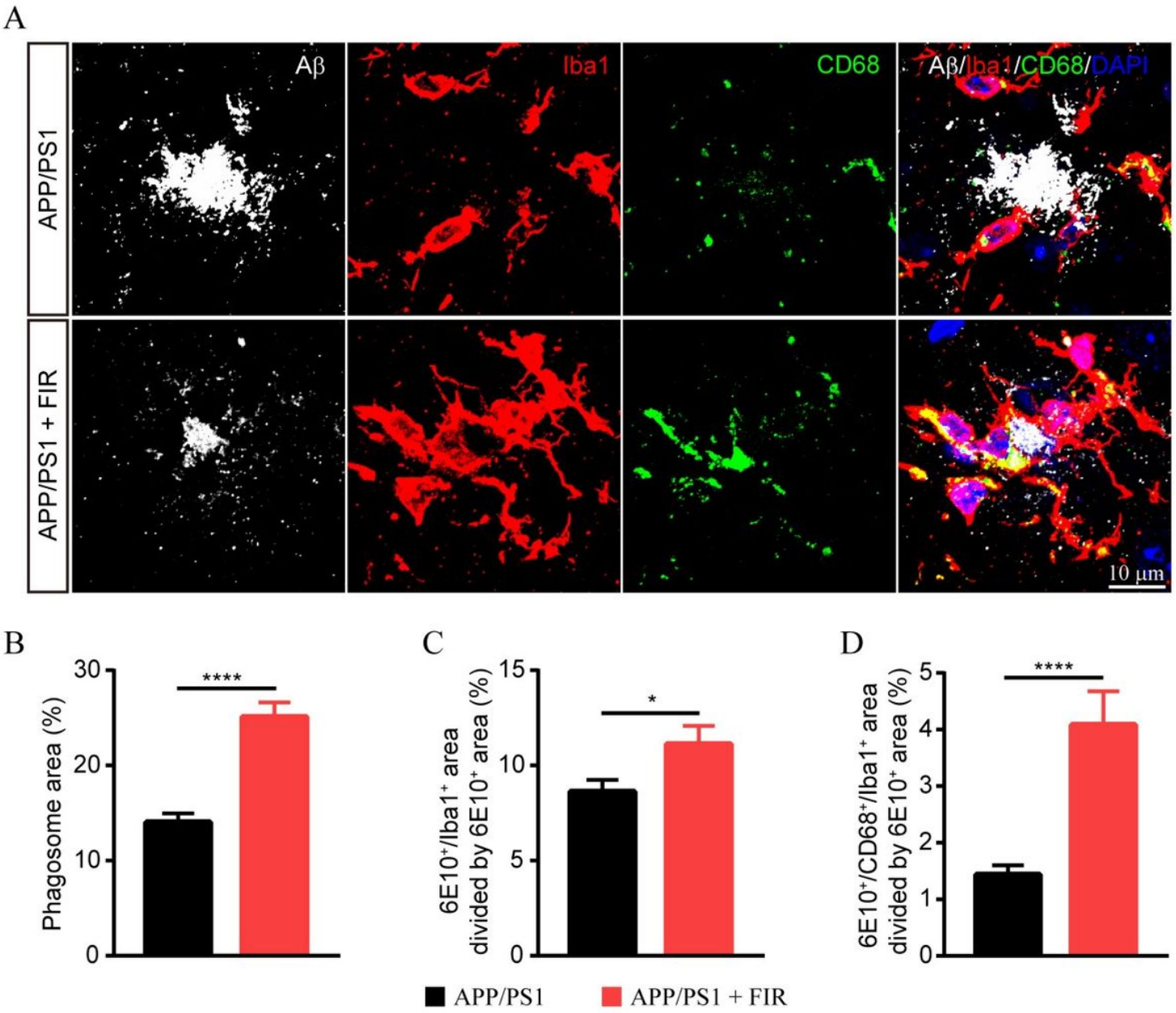

Figure 4

FIR light enhanced microglial phagocytosis of Aβ under in vivo condition. (A) Representative images of Aβ (6E10, white), microglia (Iba1, red), phagosome (CD68, green) and nuclei (DAPI, blue) co-staining in the cerebral cortex of APP/PS1 mice treated with or without FIR light. (B) Quantification of the percentage of phagosome area in Iba1 positive area. (C) Quantification of the percentage of 6E10+/Iba1+ co-staining area normalized to the total 6E10+ area. (D) Quantification of the percentage of 6E10+/CD68+/Iba1+ co-staining area normalized to the total 6E10+ area. Data were means ± S.E.M. (n = 49 - 52 per group). *P < 0.05 and ****P < 0.0001 compared to corresponding values of APP/PS1 mice without FIR light treatment.

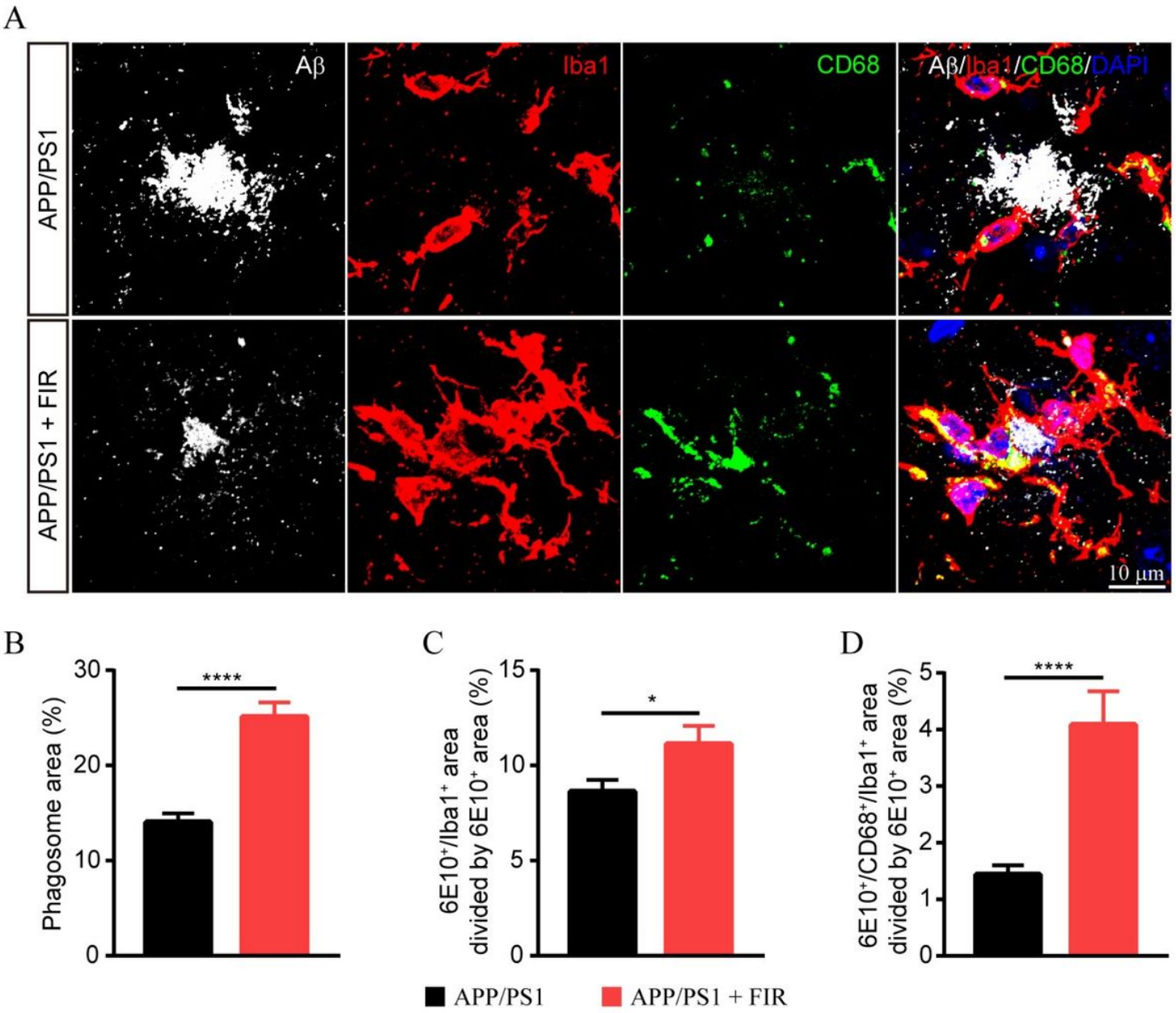

Figure 4

FIR light enhanced microglial phagocytosis of Aβ under in vivo condition. (A) Representative images of Aβ (6E10, white), microglia (Iba1, red), phagosome (CD68, green) and nuclei (DAPI, blue) co-staining in the cerebral cortex of APP/PS1 mice treated with or without FIR light. (B) Quantification of the percentage of phagosome area in Iba1 positive area. (C) Quantification of the percentage of 6E10+/Iba1+ co-staining area normalized to the total 6E10+ area. (D) Quantification of the percentage of 6E10+/CD68+/Iba1+ co-staining area normalized to the total 6E10+ area. Data were means ± S.E.M. (n = 49 - 52 per group). *P < 0.05 and ****P < 0.0001 compared to corresponding values of APP/PS1 mice without FIR light treatment.

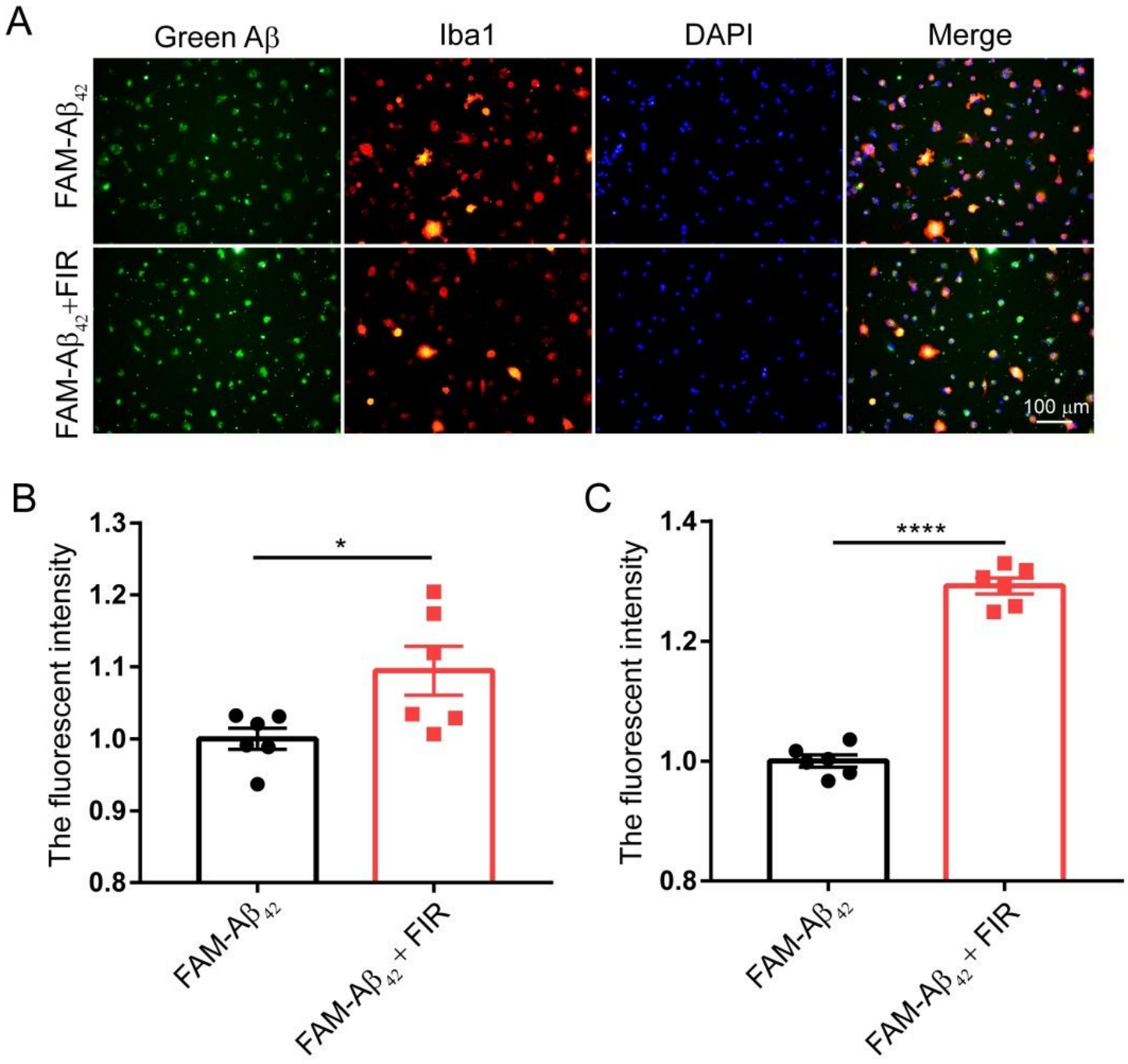

Figure 5

FIR light enhanced in vitro phagocytosis of Aβ by primary microglial cultures. (A) Representative images of the uptake of FAM-Aβ1-42. (B) Image quantification of the corresponding fluorescent intensity of FAM-Aβ1-42 engulfed by microglia (n = 6 per group). (C) Flow cytometry quantification of the fluorescent intensity of FAM-Aβ1-42 engulfed by microglia. Data were means ± S.E.M. (n = 6). *P < 0.05 and ****P < 0.0001 compared to corresponding values of microglia without FIR light treatment.

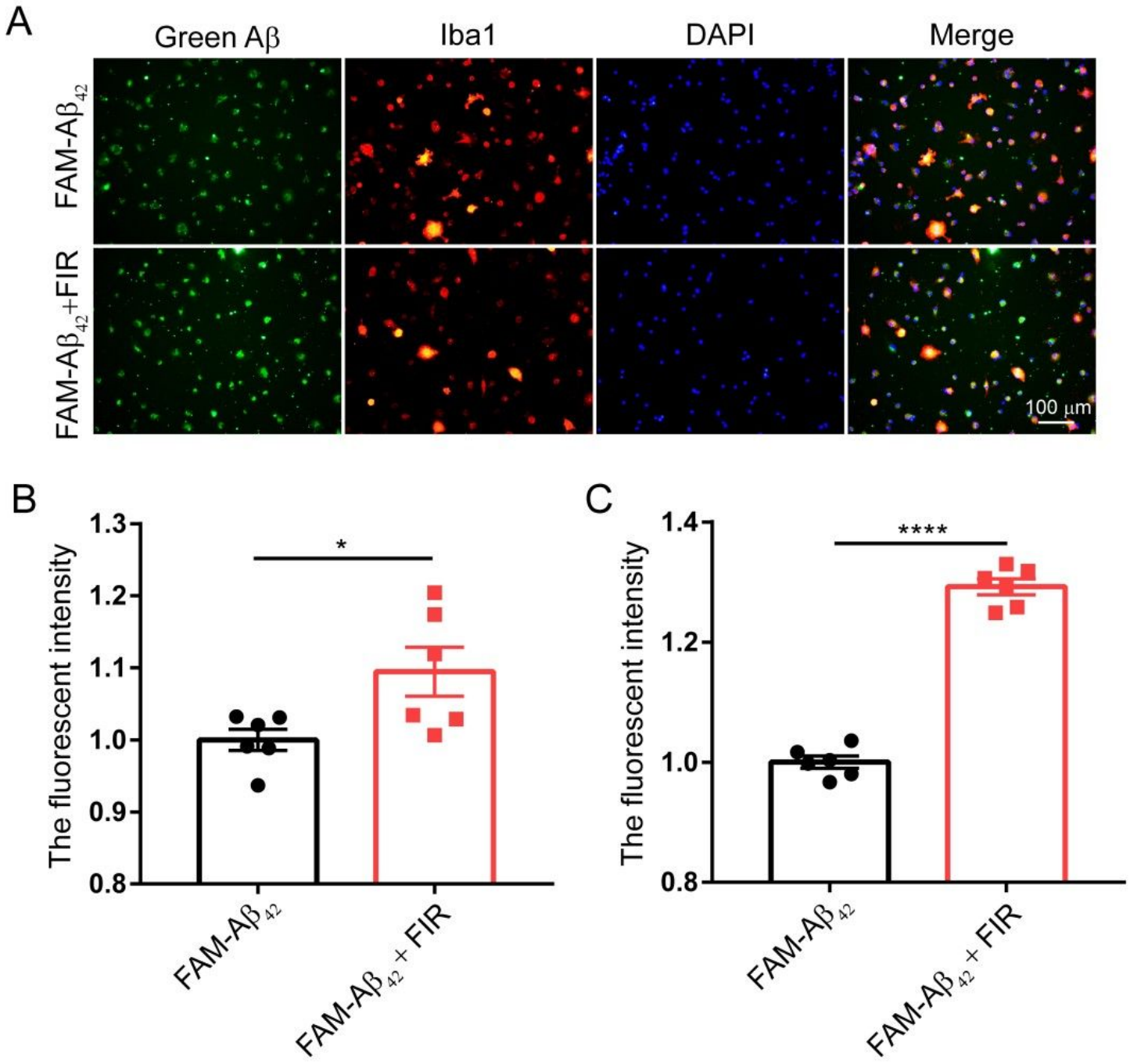

Figure 5

FIR light enhanced in vitro phagocytosis of Aβ by primary microglial cultures. (A) Representative images of the uptake of FAM-Aβ1-42. (B) Image quantification of the corresponding fluorescent intensity of FAM-Aβ1-42 engulfed by microglia (n = 6 per group). (C) Flow cytometry quantification of the fluorescent intensity of FAM-Aβ1-42 engulfed by microglia. Data were means ± S.E.M. (n = 6). *P < 0.05 and ****P < 0.0001 compared to corresponding values of microglia without FIR light treatment.

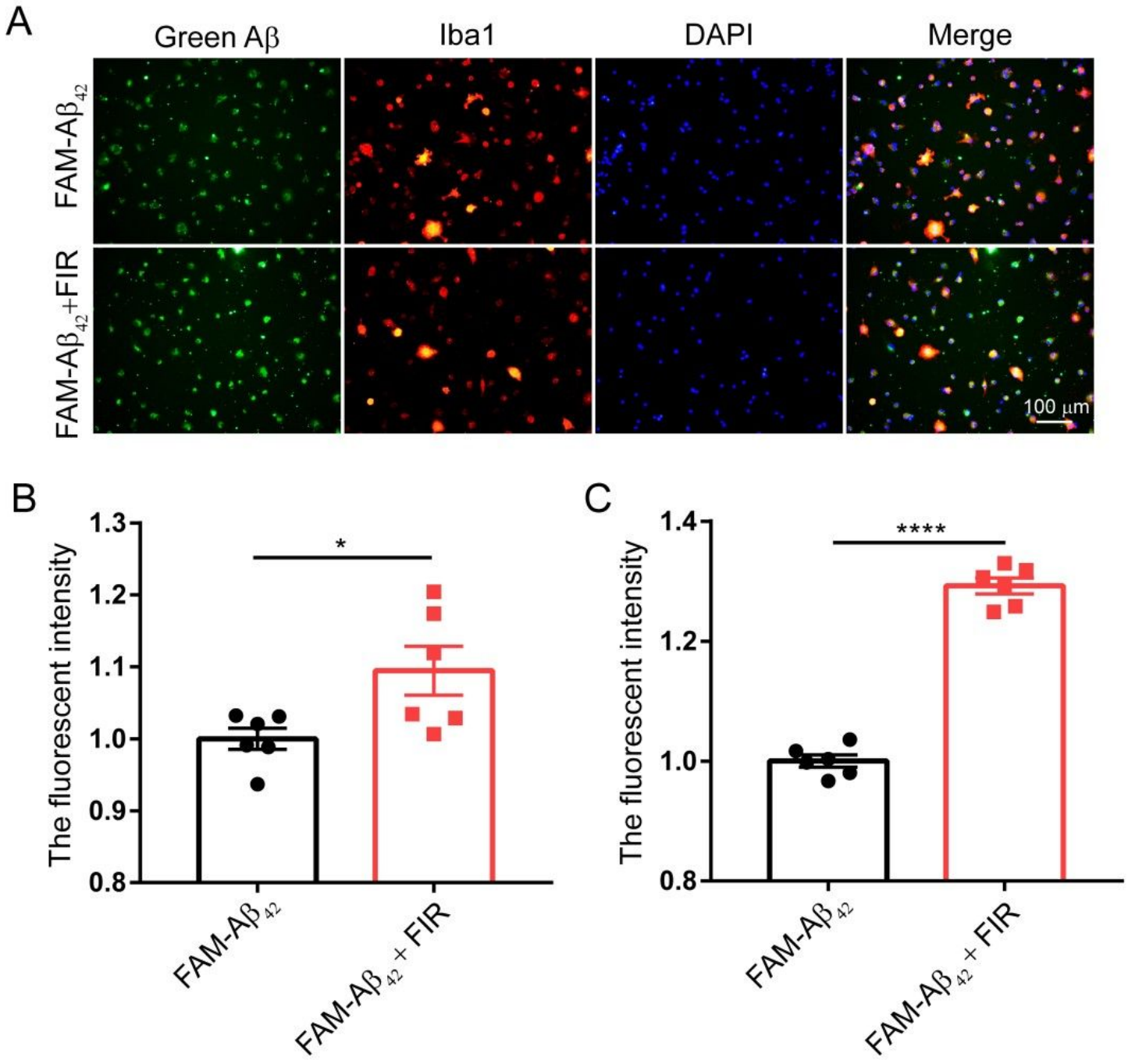

Figure 5

FIR light enhanced in vitro phagocytosis of Aβ by primary microglial cultures. (A) Representative images of the uptake of FAM-Aβ1-42. (B) Image quantification of the corresponding fluorescent intensity of FAM-Aβ1-42 engulfed by microglia (n = 6 per group). (C) Flow cytometry quantification of the fluorescent intensity of FAM-Aβ1-42 engulfed by microglia. Data were means ± S.E.M. (n = 6). *P < 0.05 and ****P < 0.0001 compared to corresponding values of microglia without FIR light treatment.

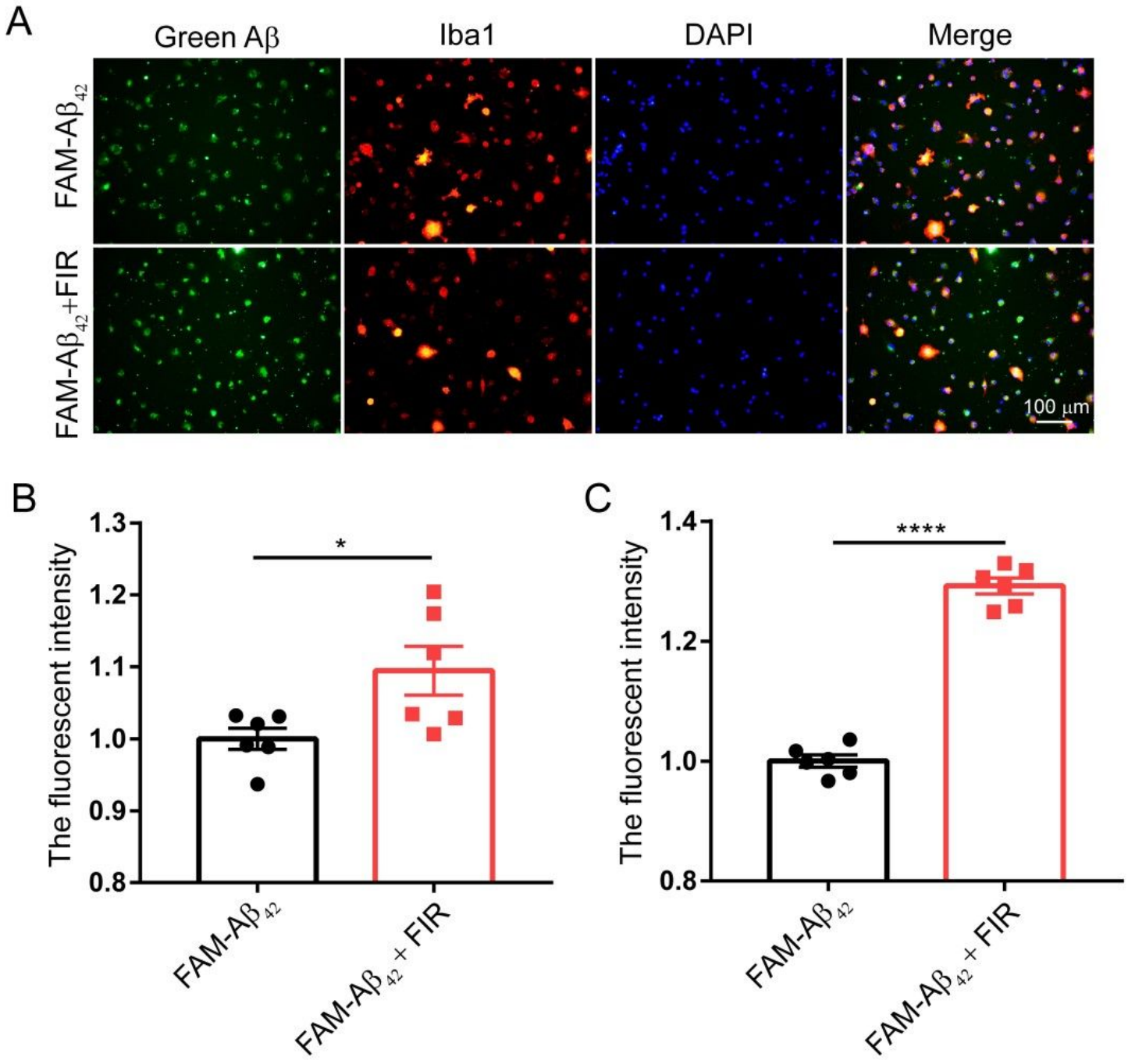

Figure 5

FIR light enhanced in vitro phagocytosis of Aβ by primary microglial cultures. (A) Representative images of the uptake of FAM-Aβ1-42. (B) Image quantification of the corresponding fluorescent intensity of FAM-Aβ1-42 engulfed by microglia (n = 6 per group). (C) Flow cytometry quantification of the fluorescent intensity of FAM-Aβ1-42 engulfed by microglia. Data were means ± S.E.M. (n = 6). *P < 0.05 and ****P < 0.0001 compared to corresponding values of microglia without FIR light treatment.

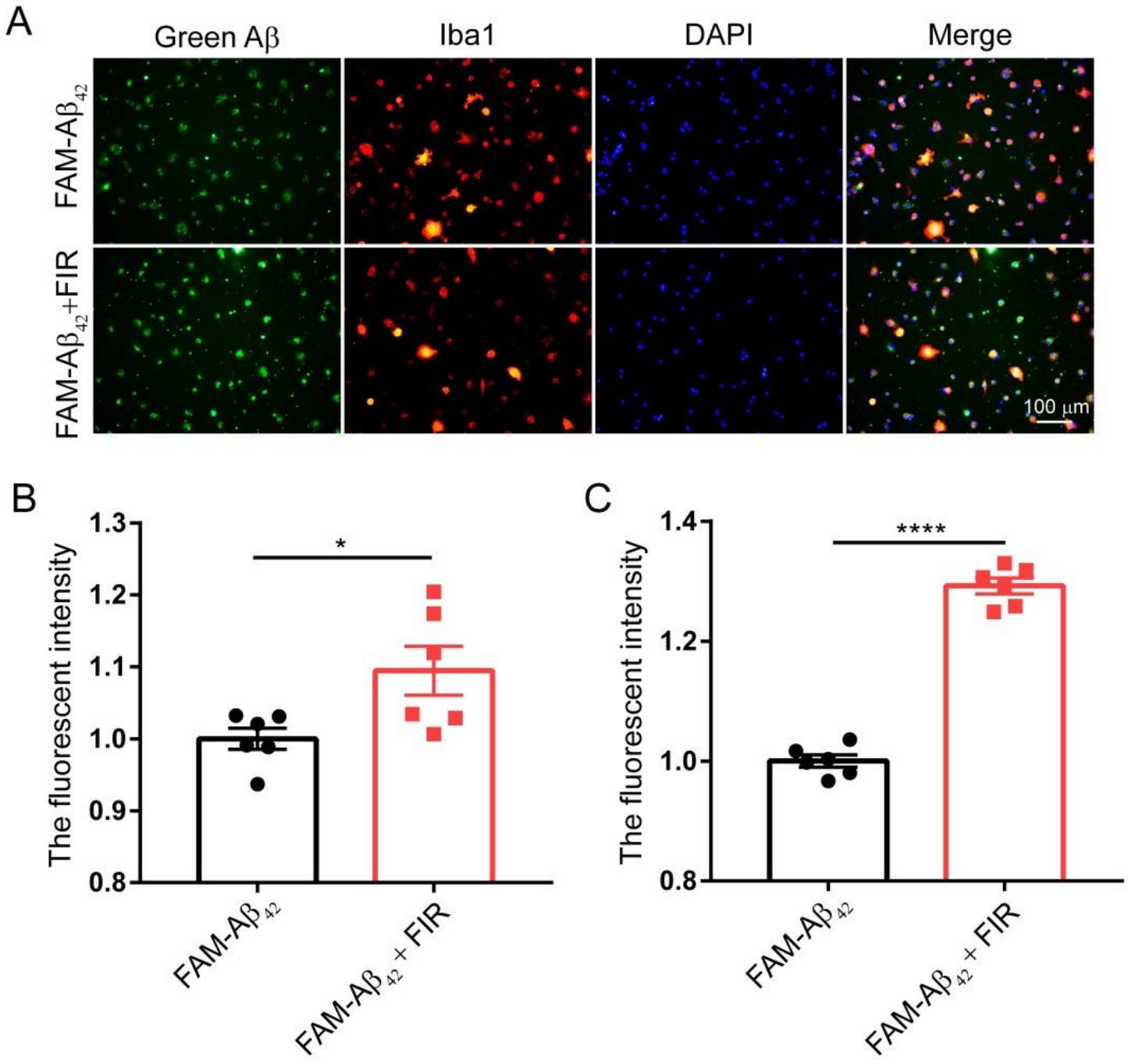

Figure 5

FIR light enhanced in vitro phagocytosis of Aβ by primary microglial cultures. (A) Representative images of the uptake of FAM-Aβ1-42. (B) Image quantification of the corresponding fluorescent intensity of FAM-Aβ1-42 engulfed by microglia (n = 6 per group). (C) Flow cytometry quantification of the fluorescent intensity of FAM-Aβ1-42 engulfed by microglia. Data were means ± S.E.M. (n = 6). *P < 0.05 and ****P < 0.0001 compared to corresponding values of microglia without FIR light treatment.

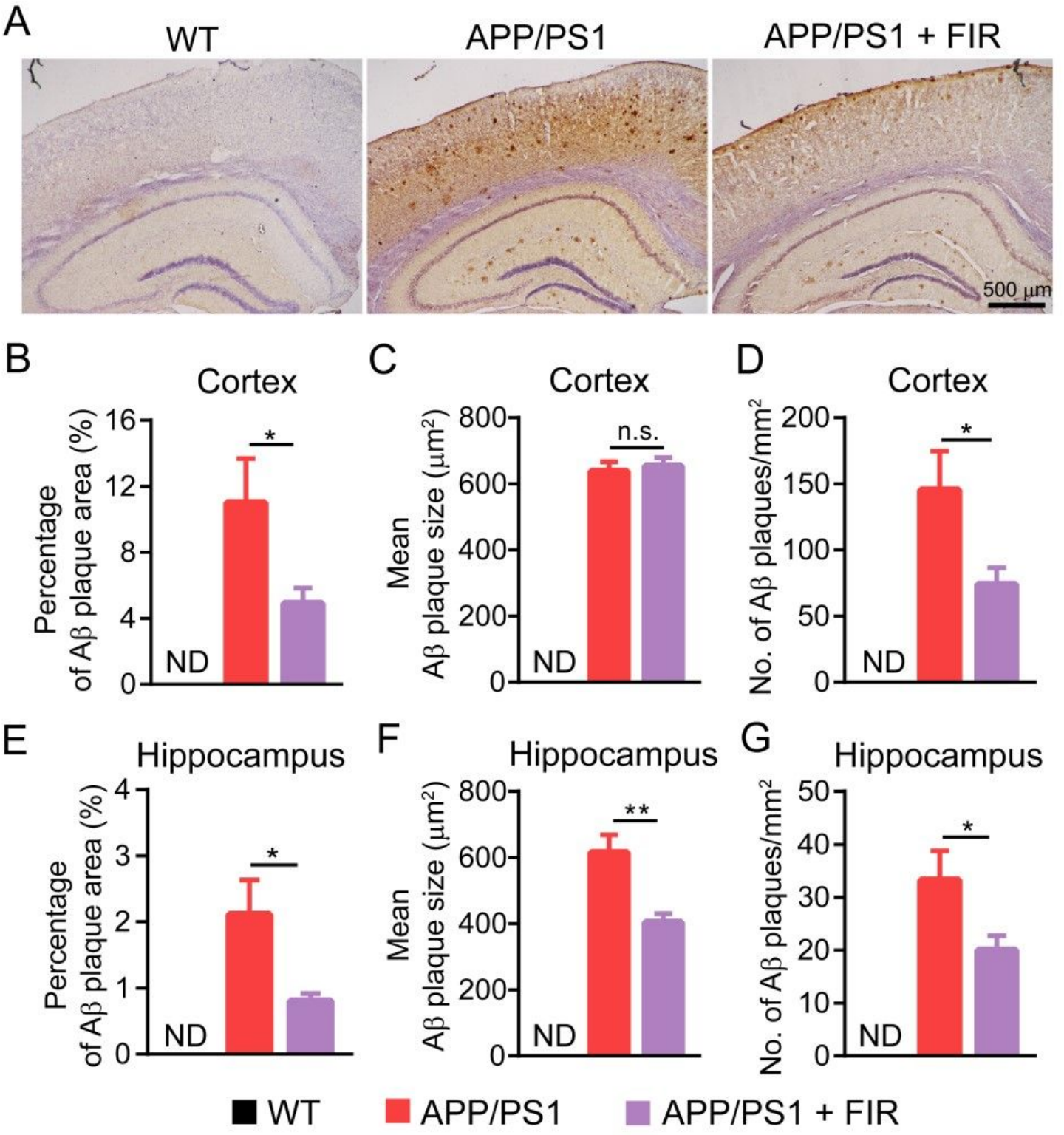

Figure 6

FIR light treatment ameliorated Aβ deposition in the cortex and hippocampus. (A) Representative images of Aβ (6E10) staining in the cerebral cortex and hippocampus from WT, APP/PS1 and FIR light-treated APP/PS1 mice. (B) Percentage of Aβ plaque area in the cerebral cortex. (C) Average size of plaques in the cerebral cortex. (D) Aβ plaque density in the cerebral cortex. (E) Percentage of Aβ plaque area in the hippocampus. (F) Average size of plaques in the hippocampus. (G) Aβ plaque density in the

hippocampus. Data were means ± S.E.M. (n = 4). *p < 0.05 and **p < 0.01 compared to corresponding values of APP/PS1 mice without FIR light treatment.

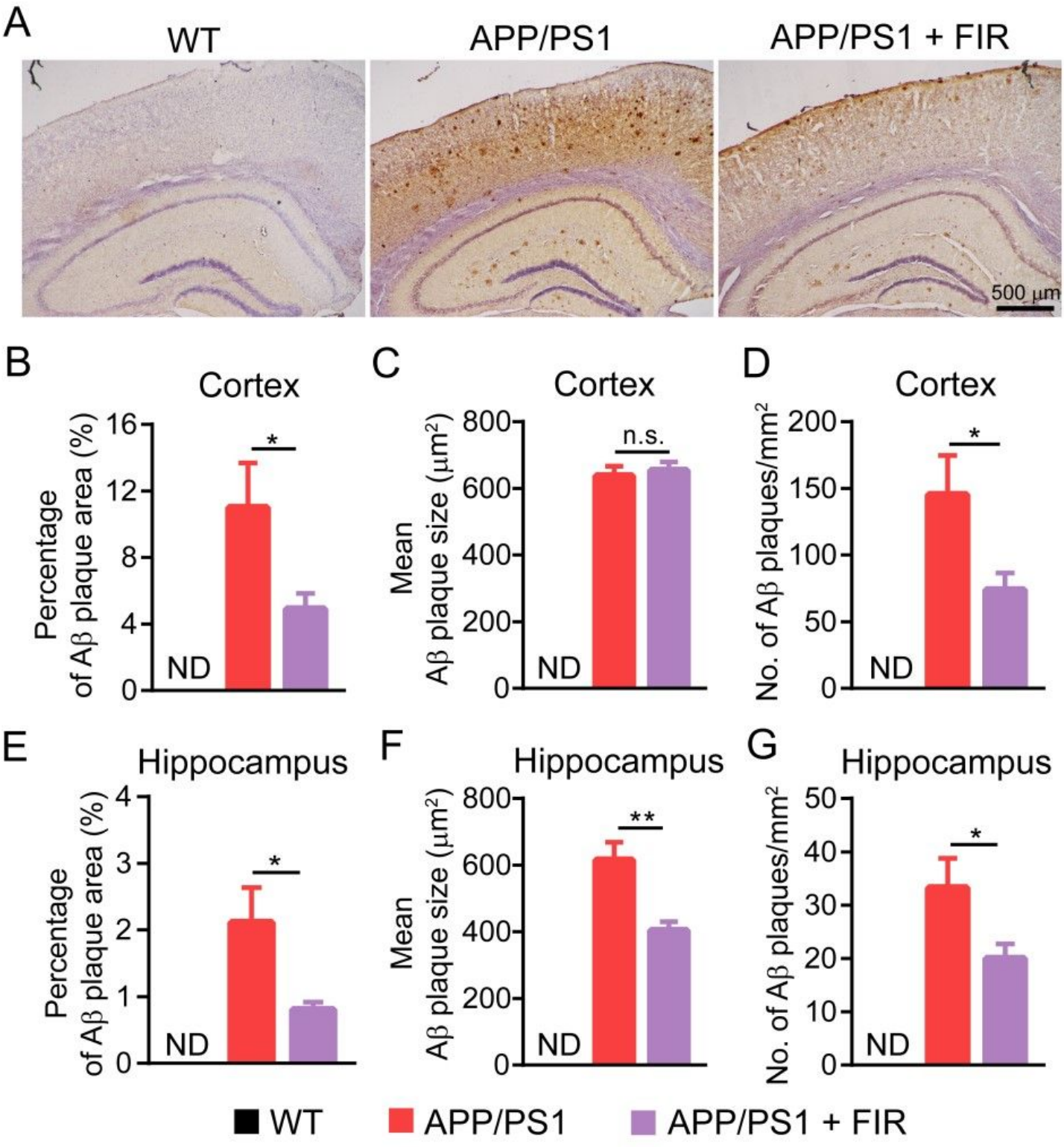

Figure 6

FIR light treatment ameliorated Aβ deposition in the cortex and hippocampus. (A) Representative images of Aβ (6E10) staining in the cerebral cortex and hippocampus from WT, APP/PS1 and FIR light-treated APP/PS1 mice. (B) Percentage of Aβ plaque area in the cerebral cortex. (C) Average size of plaques in the

cerebral cortex. (D) Aβ plaque density in the cerebral cortex. (E) Percentage of Aβ plaque area in the hippocampus. (F) Average size of plaques in the hippocampus. (G) Aβ plaque density in the hippocampus. Data were means ± S.E.M. (n = 4). *p < 0.05 and **p < 0.01 compared to corresponding values of APP/PS1 mice without FIR light treatment.

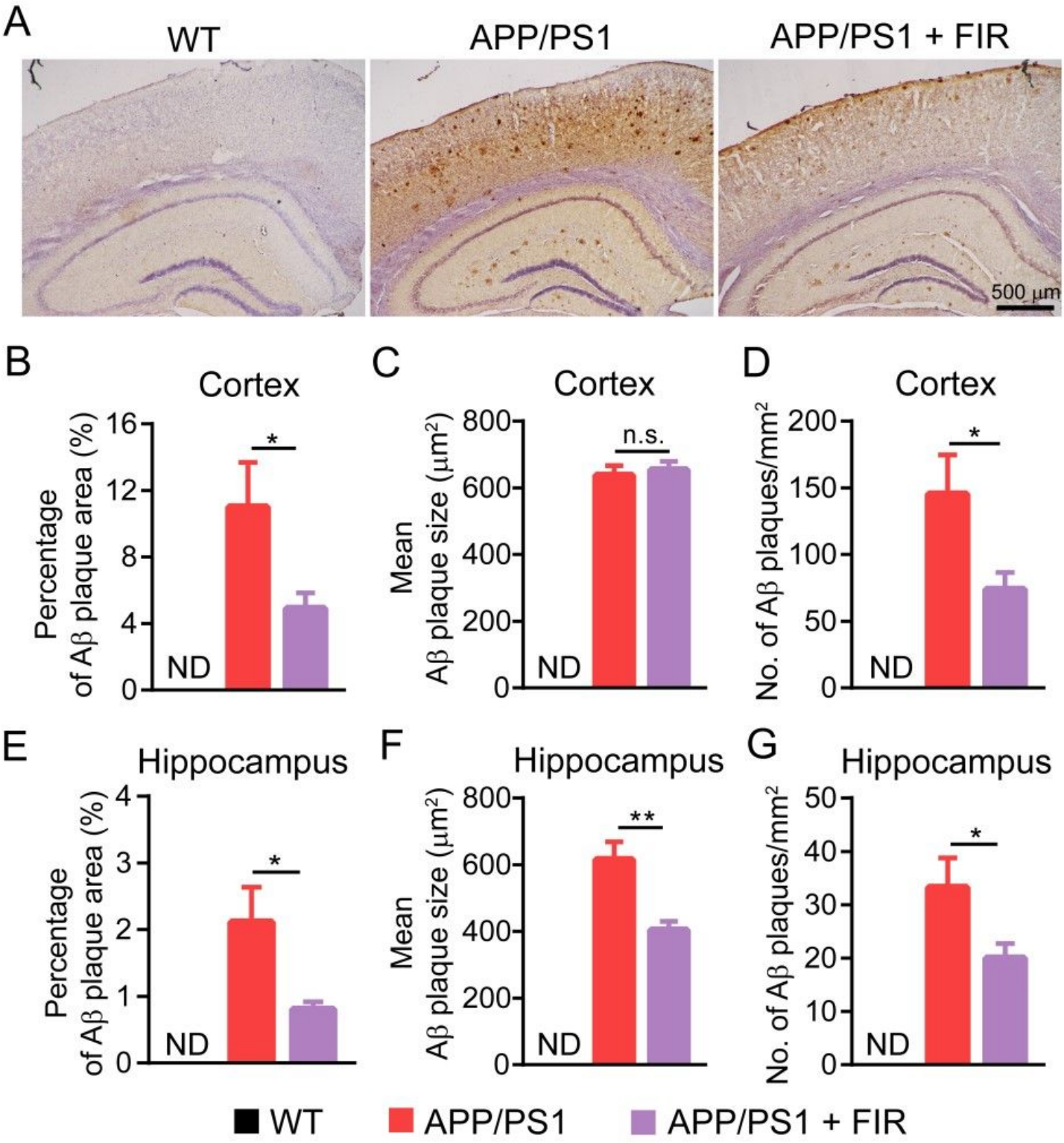

Figure 6

FIR light treatment ameliorated Aβ deposition in the cortex and hippocampus. (A) Representative images of Aβ (6E10) staining in the cerebral cortex and hippocampus from WT, APP/PS1 and FIR light-treated APP/PS1 mice. (B) Percentage of Aβ plaque area in the cerebral cortex. (C) Average size of plaques in the cerebral cortex. (D) Aβ plaque density in the cerebral cortex. (E) Percentage of Aβ plaque area in the hippocampus. (F) Average size of plaques in the hippocampus. (G) Aβ plaque density in the hippocampus. Data were means ± S.E.M. (n = 4). *p < 0.05 and **p < 0.01 compared to corresponding values of APP/PS1 mice without FIR light treatment.

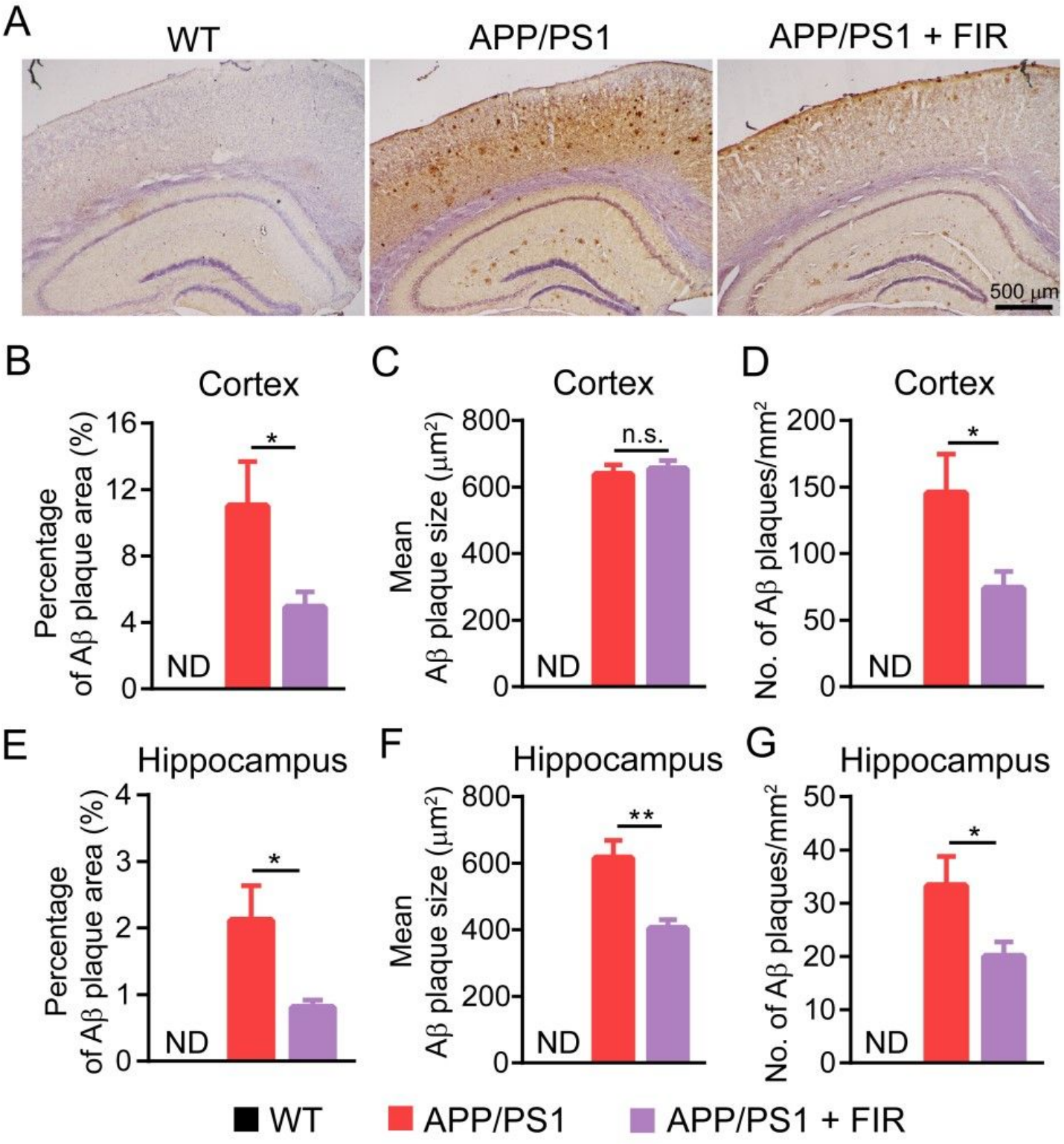

Figure 6

FIR light treatment ameliorated Aβ deposition in the cortex and hippocampus. (A) Representative images of Aβ (6E10) staining in the cerebral cortex and hippocampus from WT, APP/PS1 and FIR light-treated APP/PS1 mice. (B) Percentage of Aβ plaque area in the cerebral cortex. (C) Average size of plaques in the cerebral cortex. (D) Aβ plaque density in the cerebral cortex. (E) Percentage of Aβ plaque area in the hippocampus. (F) Average size of plaques in the hippocampus. (G) Aβ plaque density in the hippocampus. Data were means ± S.E.M. (n = 4). *$p < 0.05$ and **$p < 0.01$ compared to corresponding values of APP/PS1 mice without FIR light treatment.

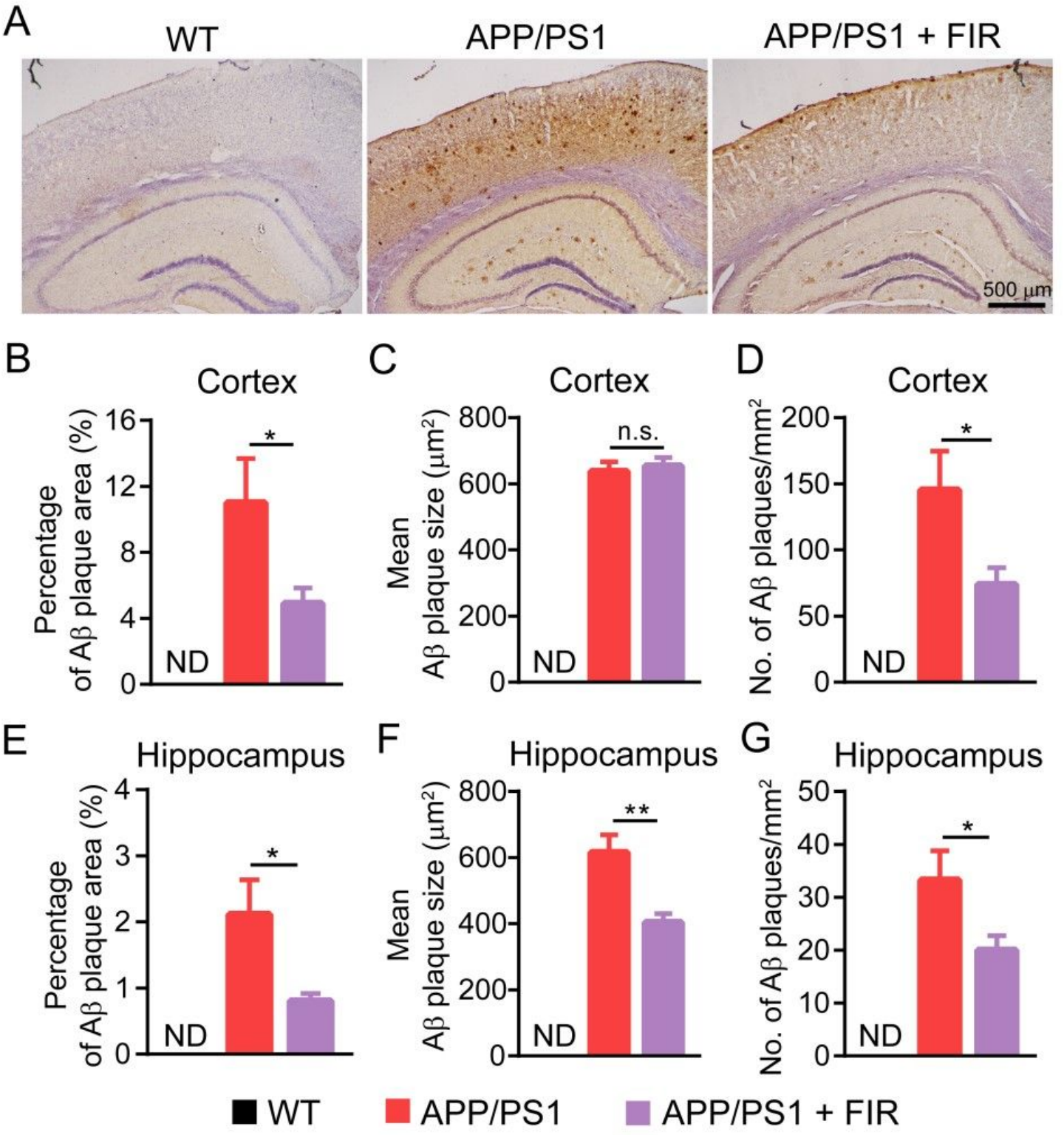

Figure 6

FIR light treatment ameliorated Aβ deposition in the cortex and hippocampus. (A) Representative images of Aβ (6E10) staining in the cerebral cortex and hippocampus from WT, APP/PS1 and FIR light-treated APP/PS1 mice. (B) Percentage of Aβ plaque area in the cerebral cortex. (C) Average size of plaques in the cerebral cortex. (D) Aβ plaque density in the cerebral cortex. (E) Percentage of Aβ plaque area in the hippocampus. (F) Average size of plaques in the hippocampus. (G) Aβ plaque density in the

hippocampus. Data were means ± S.E.M. (n = 4). *p < 0.05 and **p < 0.01 compared to corresponding values of APP/PS1 mice without FIR light treatment.

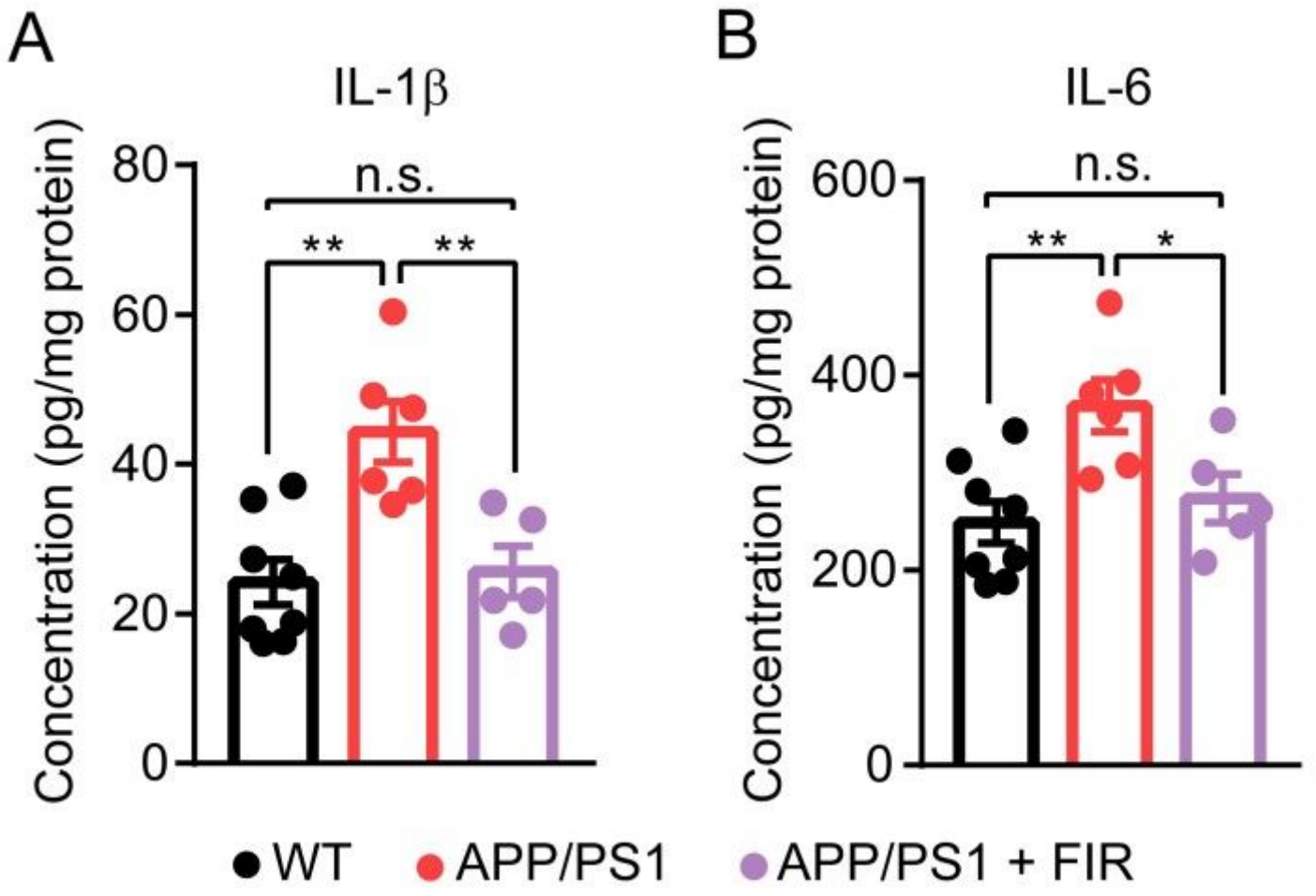

Figure 7

FIR light treatment alleviated neuroinflammation in the AD-like mice. (A) IL-1β levels in the cerebral cortex. (B) IL-6 levels in the cerebral cortex. Data were means ± S.E.M. (n = 5 - 8 per group) *P < 0.05 and **p < 0.01 compared to corresponding values of APP/PS1 mice without FIR light treatment.

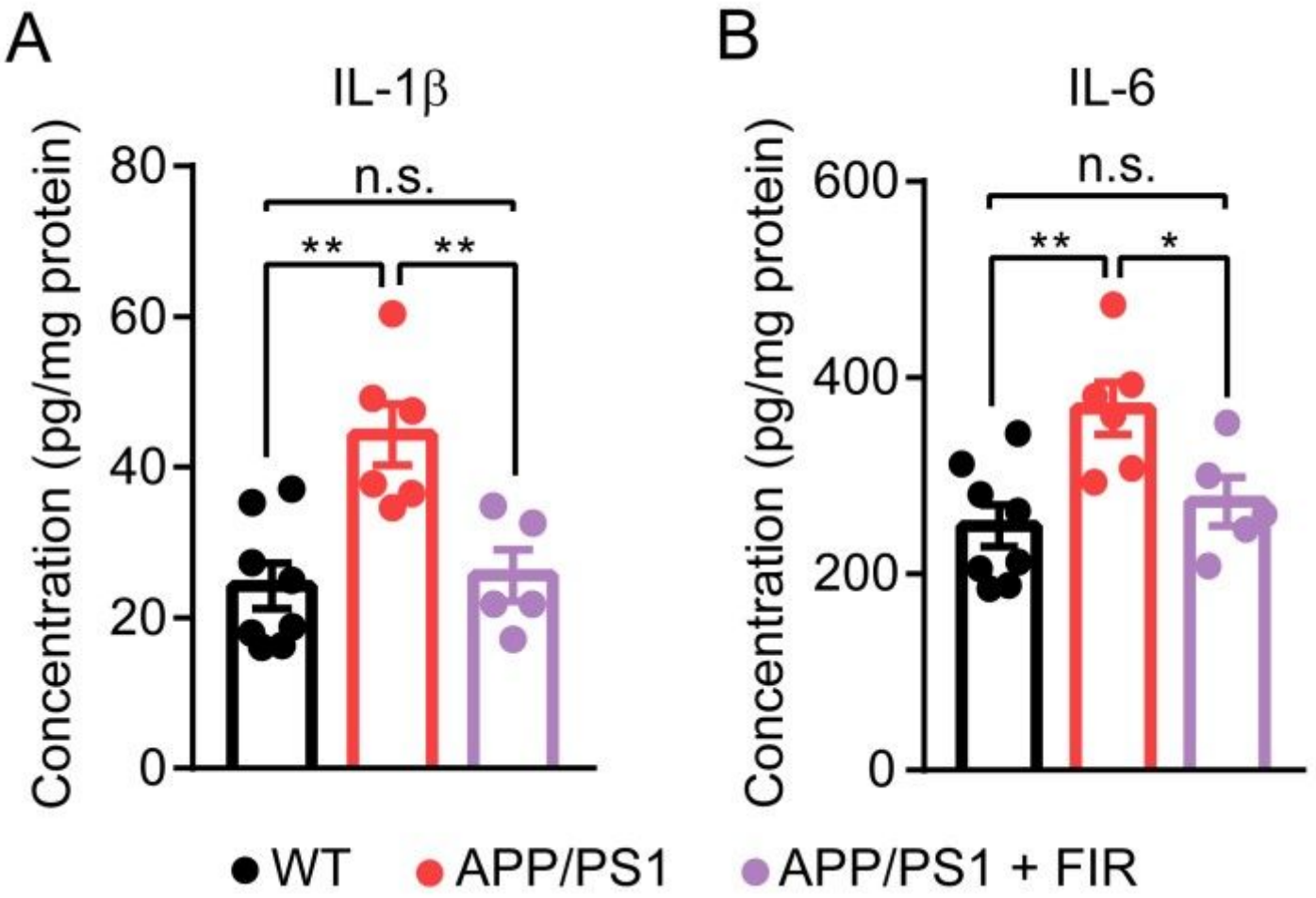

Figure 7

FIR light treatment alleviated neuroinflammation in the AD-like mice. (A) IL-1β levels in the cerebral cortex. (B) IL-6 levels in the cerebral cortex. Data were means ± S.E.M. (n = 5 - 8 per group) *P < 0.05 and **p < 0.01 compared to corresponding values of APP/PS1 mice without FIR light treatment.

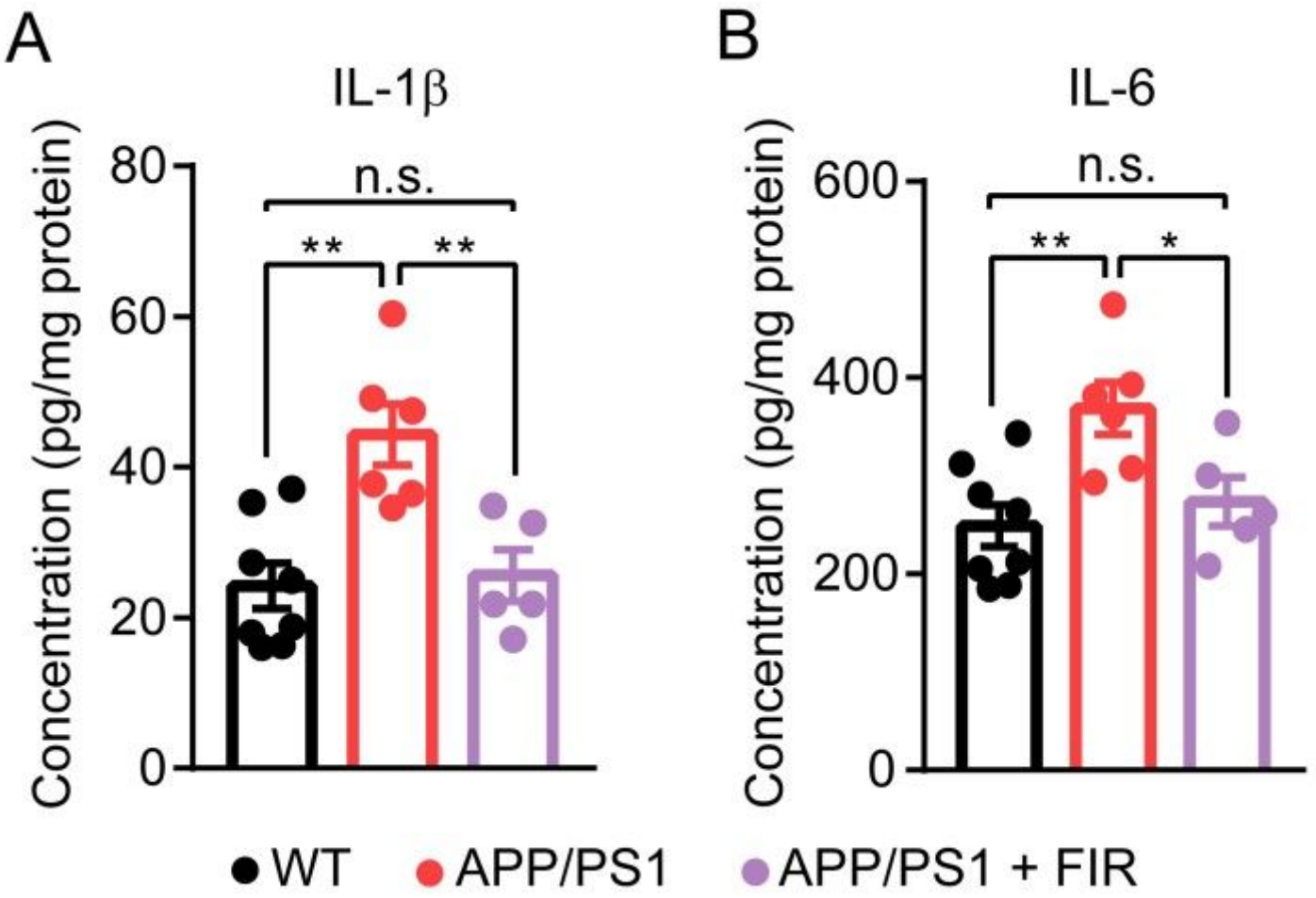

Figure 7

FIR light treatment alleviated neuroinflammation in the AD-like mice. (A) IL-1β levels in the cerebral cortex. (B) IL-6 levels in the cerebral cortex. Data were means ± S.E.M. (n = 5 - 8 per group) *P < 0.05 and **p < 0.01 compared to corresponding values of APP/PS1 mice without FIR light treatment.

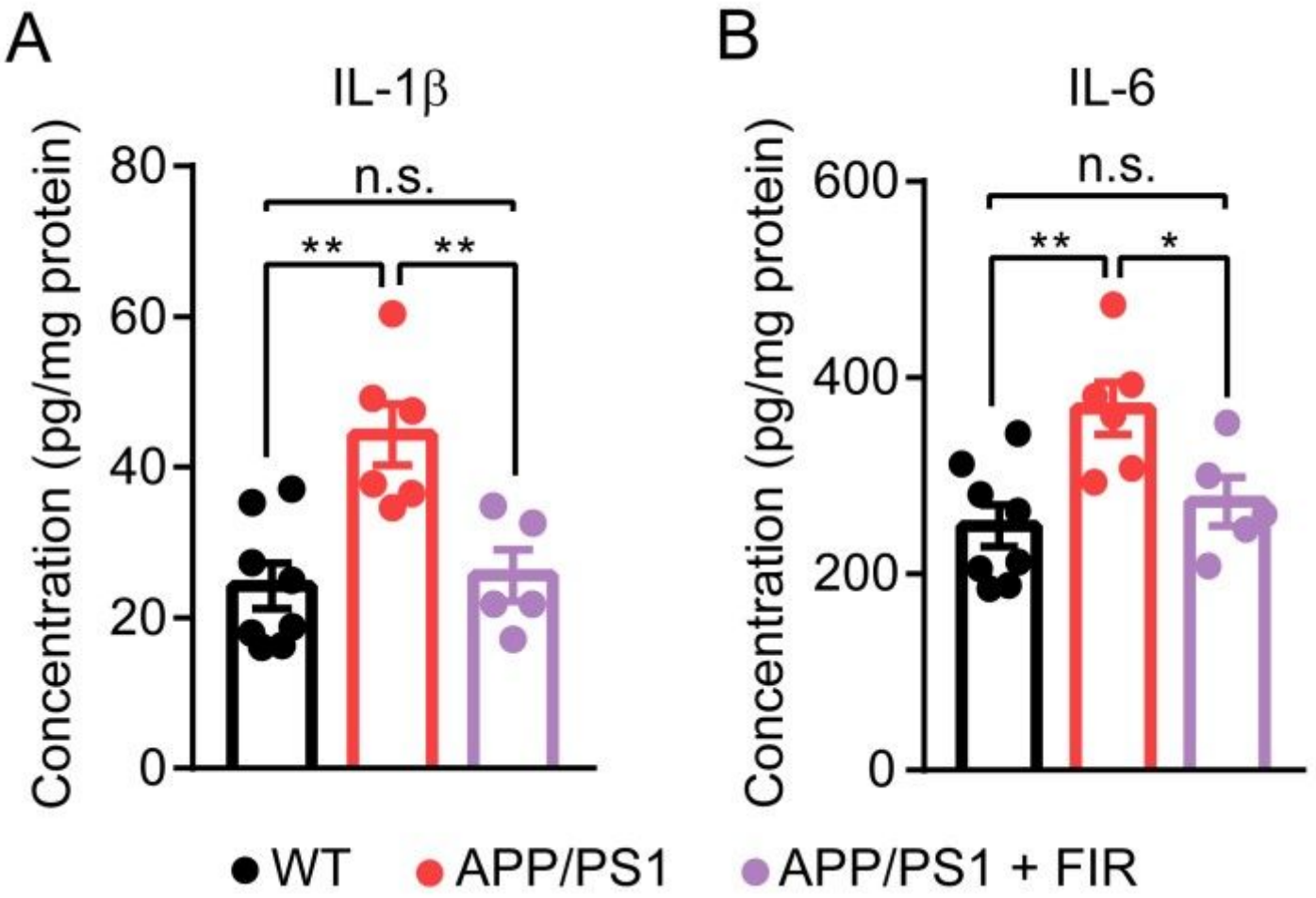

Figure 7

FIR light treatment alleviated neuroinflammation in the AD-like mice. (A) IL-1β levels in the cerebral cortex. (B) IL-6 levels in the cerebral cortex. Data were means ± S.E.M. (n = 5 - 8 per group) *P < 0.05 and **p < 0.01 compared to corresponding values of APP/PS1 mice without FIR light treatment.

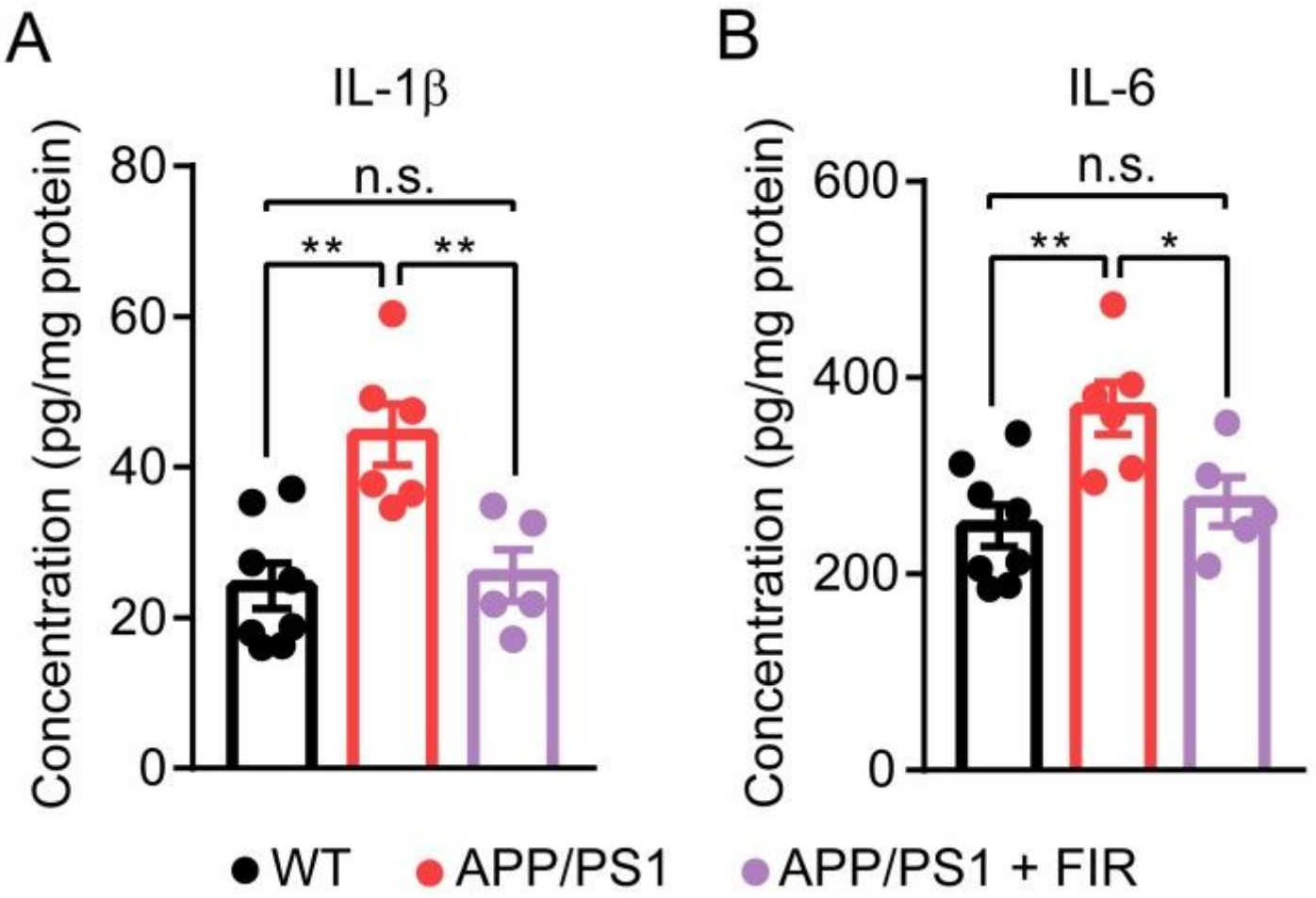

Figure 7

FIR light treatment alleviated neuroinflammation in the AD-like mice. (A) IL-1β levels in the cerebral cortex. (B) IL-6 levels in the cerebral cortex. Data were means ± S.E.M. (n = 5 - 8 per group) *P < 0.05 and **p < 0.01 compared to corresponding values of APP/PS1 mice without FIR light treatment.